batteries

MDPI

Review

Sodium Polymer Electrolytes: A Review

Sumit Kumar [1,2], Rajesh Raghupathy [1,3] and Michele Vittadello [1,4,5,*]

[1] Department of Chemistry and Environmental Science, Medgar Evers College, City University of New York (CUNY), 1638 Bedford Avenue, Brooklyn, NY 11225, USA; skumar9@chemistry.du.ac.in (S.K.)
[2] Bioorganic Research Laboratory, Department of Chemistry, University of Delhi, University Enclave, Delhi 110007, India
[3] Nano and Bioelectrochemistry Research Laboratory, Carbon Dioxide Research and Green Technology Centre, Department of Chemistry, School of Advanced Sciences, Vellore Institute of Technology, Turuvalam Road, Vellore 632014, India
[4] Ph.D. Program in Chemistry, The Graduate Center of CUNY, 365 5th Avenue, New York, NY 10016, USA
[5] M.S. Program in Nanoscience, The Graduate Center of CUNY, 365 5th Avenue, New York, NY 10016, USA
* Correspondence: mvittadello@mec.cuny.edu

Abstract: Lithium-based electrolytes are, at least from a thermodynamic standpoint, the most suitable ion-transport materials for energy storage systems. However, lithium-based ionic conductors suffer from safety concerns, and the limited availability of lithium in the Earth's crust is at the root of the need to consider alternative metal ions. Notably, sodium stands out as the sixth most-prevalent element; therefore, when considering mineral reserves, it as a very attractive candidate as an alternative to the status quo. Even if the specific energy and energy density of sodium are indeed inferior with respect to those of lithium, there is substantial economic appeal in promoting the use of the former metal in stationary energy storage applications. For these reasons, the promise of sodium is likely to extend to other commercial applications, including portable electronics, as well as hybrid and electric vehicles. Widely used organic liquid electrolytes, regardless of their chosen metal cation, are disadvantageous due to leakage, evaporation, and high flammability. Polymer electrolytes are acknowledged as the most effective candidates to overcome these obstacles and facilitate the advancement of next-generation energy storage applications. In this contribution, an in-depth and comprehensive review of sodium polymer electrolytes for primary and secondary batteries is proposed. The overarching goal was to gain insight into successful synthetic strategies and their implications for conduction parameters and conductivity mechanisms. The focus lies on solid, gel, and composite polymer electrolytes. Our hope is that the proposed discussion will be helpful to all operators in the field, whether in tackling fundamental research problems or resolving issues of practical significance.

Keywords: sodium polymer electrolytes; sodium solid polymer electrolytes; sodium gel polymer electrolytes; sodium composite polymer electrolytes; sodium ion batteries

Citation: Kumar, S.; Raghupathy, R.; Vittadello, M. Sodium Polymer Electrolytes: A Review. *Batteries* **2024**, *10*, 73. https://doi.org/10.3390/batteries10030073

Academic Editor: Jun Yan

Received: 3 November 2023
Revised: 13 February 2024
Accepted: 16 February 2024
Published: 21 February 2024

1. Introduction

In recent years, there has been an escalating worldwide effort to transition from a global energy system reliant on hydrocarbons to one based on carbon-neutral alternatives. A consequent epochal shift is underway, which has been gaining significant momentum and is often characterized as the grand challenge of our times. Given the limited availability of conventional fossil fuels, renewable energy sources such as wind, solar, and nuclear energy solutions have grown in importance [1]. However, the cyclical nature and uneven spatial distribution of the first two types of renewable energy resources prevent them from constituting a constant power supply. In contrast, nuclear energy is still considered too dangerous to be fully reliable. Regardless of the preferred energy solution mixture, stable and dependable energy storage will be a crucial part of the expected economic shift. Batteries are anticipated to claim a sizable share of the energy market, even though it is yet unclear which combination of energy storage technologies will prevail. As a

result, significant emphasis has been placed on research and development in this field. Rechargeable batteries are endowed with sufficient versatility to store energy and efficiently turn it into usable power [2]. Lithium-ion batteries (LIBs) have historically held a dominant position in the markets of portable electronics, electric vehicles, and hybrid vehicles due to their impressive performance parameters, such as high output voltages, substantial energy densities, and extended cycle lives. Nonetheless, the elevated costs of extraction and finite availability of lithium reserves impose constraints on the widespread adoption of LIBs for large-scale energy storage applications [3–5].

Due to the scarcity of earth deposits and unequal distribution of lithium resources (with 70% of known mineral reserves being located in South America), future commercial applications of LIBs are hampered by high costs and environmental concerns [6,7]. The availability of lithium resources has nearly doubled since 1991 [8,9], which is beneficial for commercial applications. Given the redox potential of sodium (−2.71 V vs. SHE, a mere 0.3 V higher than that of lithium), abundant sodium resources, and cost-effective sodium salts, sodium-ion batteries (SIBs) have garnered significant interest. Research in SIBs has continued to increase exponentially, other than some appreciable slow-down during the COVID-19 pandemic, as shown in Figure 1 [10].

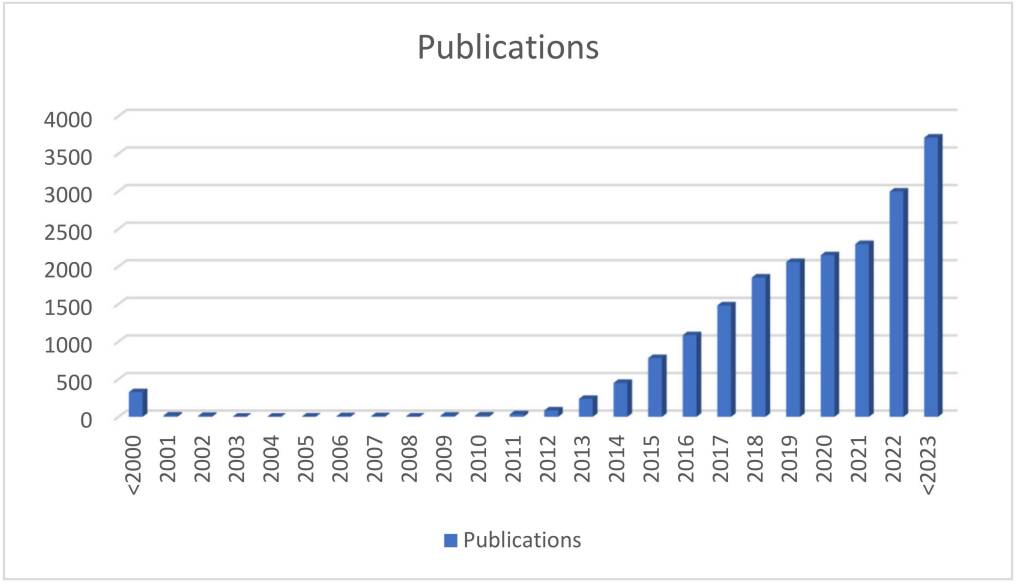

Figure 1. Number of publications on sodium batteries over time.

SIBs are expected to emerge as strong contenders in stationary energy storage applications, even though LIBs are predicted to maintain dominance in conditions where energy density takes precedence [11]. Since Na atoms are larger and heavier than Li atoms, it is inevitable that the energy density of SIBs will never be higher than that of Li power sources [12]. However, in the context of large-scale electrical grid support, battery distribution and durability are the most crucial factors, not energy density [13]. Since lithium and sodium are both alkali metals, they exhibit similar chemistries, and their electrochemical processes in SIBs and LIBs are almost an exact match. These characteristics have sped up the development of SIBs to the point that they now have a high enough energy density to replace LIBs in many applications. SIBs generally consist of two electrodes, which are comprised of thin metallic current collectors coated with active materials for both the anodes and cathodes. These electrodes are interfaced with a non-aqueous liquid electrolyte, and a thin separator sheet, typically constructed from polyolefin or fiberglass, is used to keep them apart. Despite their competitive characteristics, SIBs have not yet gained significant commercial acceptance [14].

However, an important milestone in practical SIBs was recently achieved by Yang et al. [15]. SIBs were used to power 120 Wh/kg low-speed electric vehicles, suggesting

the impending widespread commercialization of SIBs. There have been substantial efforts addressed at developing cathode and anode active materials for SIBs with a variety of operating voltage ranges and reversible capabilities [16–18].

Presently available carbonate-based lithium-ion electrolytes, known for their high ionic conductivity and elevated dielectric constants, unfortunately suffer from flammability, inadequate thermal stability, and the propensity for leakage. There are valuable lessons to be learned from incidents involving burning consumer electronics powered by LIBs (as exemplified by the Samsung Galaxy Note 7 smartphones), primarily attributable to the use of liquid electrolytes. Conventional liquid electrolyte-based SIBs continue to be plagued by weighty disadvantages, including unfavorable interactions between electrodes and electrolytes, the inevitable formation of sodium dendrites, and associated safety concerns.

In response to the challenges affecting liquid electrolytes, researchers have explored alternative electrolyte options for high-performance SIBs. Among these, inorganic solid electrolytes stand out for their high ionic conductivities (>10^{-4} S·cm^{-1}) and enhanced thermal stability. However, these materials do present difficulties related to processability and compatibility with electrode interfaces [19,20]. Among the possible solutions, polymer electrolytes (PEs) exhibit exceptional properties that make them ideal for use in SIBs, including the absence of liquid leakage, minimal flammability, high processability in a variety of formats, and outstanding flexibility [21,22].

PEs are categorized primarily into three distinct groups: solid polymer electrolytes (SPEs), gel polymer electrolytes (GPEs), and composite polymer electrolytes (CPEs), as illustrated in Figure 2.

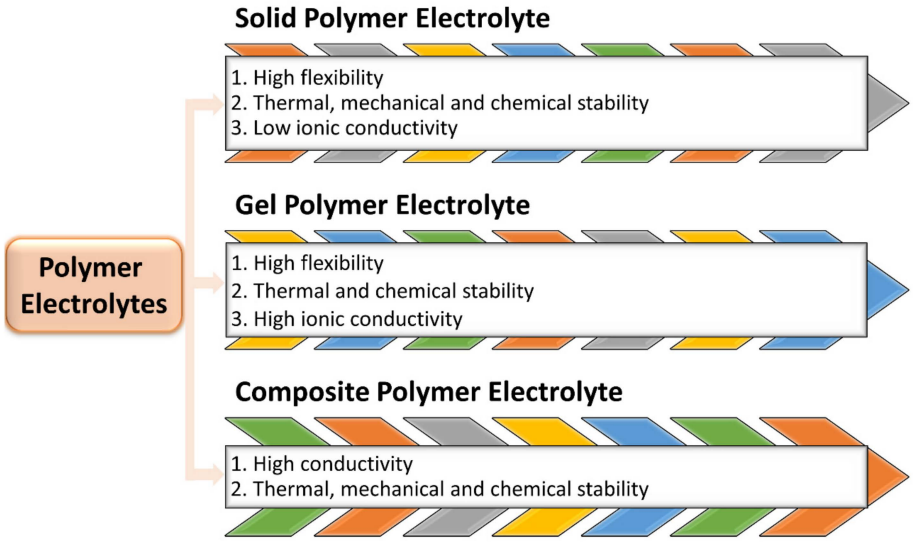

Figure 2. Classifications of polymer electrolytes.

The main benefits of PEs are related to their low processing costs. These electrolytic materials can be synthesized at relatively low temperatures, are considerably more likely to exhibit air stability, and can effectively undergo roll-to-roll production processes. Moreover, the interface between the electrode and electrolyte is typically stabilized by PEs, increasing their effective conductivity. The most practical route to all-solid-state batteries may be provided by PEs due to their combined benefits in terms of processability and performance. However, a number of issues still need to be resolved before their practical use is economically viable. Especially at or below room temperature, the conductivity of SPEs tends to be insufficient for practical real-world applications. Reports on sodium-based batteries date back to the same time as lithium-based batteries [23,24]. During the 1990s, these technologies were largely overlooked due to the emergence of commercially available lithium-based batteries, including Li–MoS_2 and Li–Li_xMnO_2 systems [25]. In the SIB system, sodium ions (Na^+) shuttle back and forth between the two electrodes as the

battery charges and discharges, giving rise to a "rocking-chair" mechanism. During the charging phase, Na^+ ions deintercalate from the cathode, diffuse through the electrolyte, and subsequently intercalate within the anode material. The process of discharge is the opposite phenomenon. In principle, the electrochemical window of a cell can be inferred by considering the LUMO and HOMO energies that are intrinsic to the electrolyte. In this contribution, we evaluated the main electrolyte categories, with special attention to current research progress relevant to SIBs.

Recent developments in battery-based electrochemical energy storage (EES) technologies are showing substantial progress. These technologies offer attractive features such as a high round-trip efficiency, adaptable power, energy characteristics suitable for various grid applications, a long cycle life, and cost-effective maintenance. The electrolyte must be endowed with chemical and electrochemical stability when in contact with both the cathode and anode surfaces. During operation, the electrolyte should remain chemically unaltered, and all Faradaic reactions should occur within the electrodes [26,27].

Due to their high energy and power density, rechargeable LIBs have been the subject of significant research. Nevertheless, the shortcomings of this technology, such as cost, limited lithium resources, dependability, and safety, are readily apparent. Figure 3 illustrates the relative quantity of different elements in the Earth's crust. The relative abundance of lithium is restricted to 20 parts per million. In fact, the cost of key ingredients (the price of $LiCoO_2$) climbed dramatically throughout the first decade of this century and continues to rise to this day. In an effort to address the challenges mentioned above, extensive research has been conducted in the field of rechargeable batteries. These studies have focused on identifying host materials capable of efficiently mobilizing guest ions beyond lithium. These include monovalent ions such as Na^+ and K^+, as well as multivalent cations such as Mg^{2+}, Ca^{2+}, Zn^{2+}, and Al^{3+}. The abundance of sodium in the Earth's crust is significantly higher compared to lithium, with sodium at 2.36% and lithium at 0.01%.

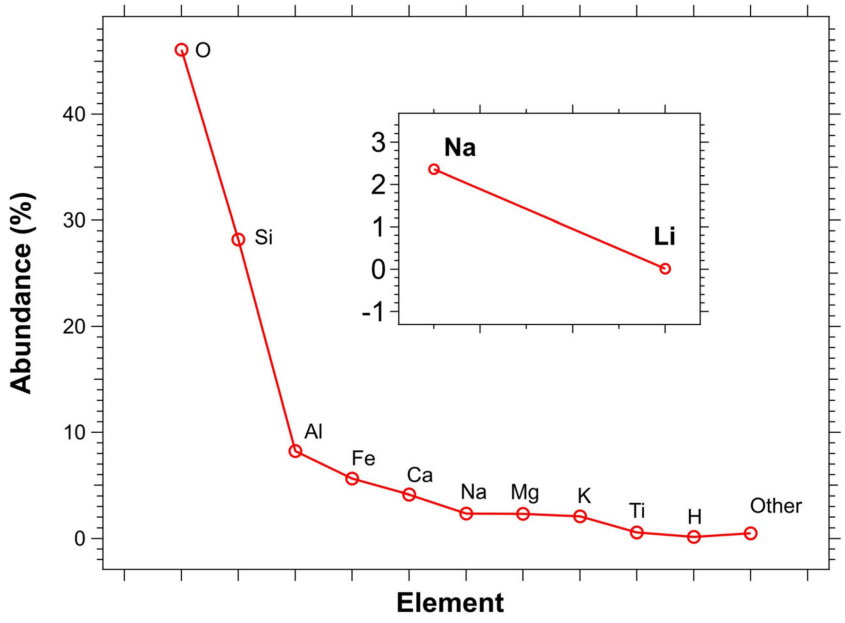

Figure 3. Elemental abundance in the Earth's crust (see also ref. [28]).

Due to the aforementioned potential disadvantages associated with LIBs, it is imperative to consider SIBs as an alternative [29]. Thus far, significant research has been conducted in an effort to optimize the electrodes, the electrolyte, and the binder (Figure 4).

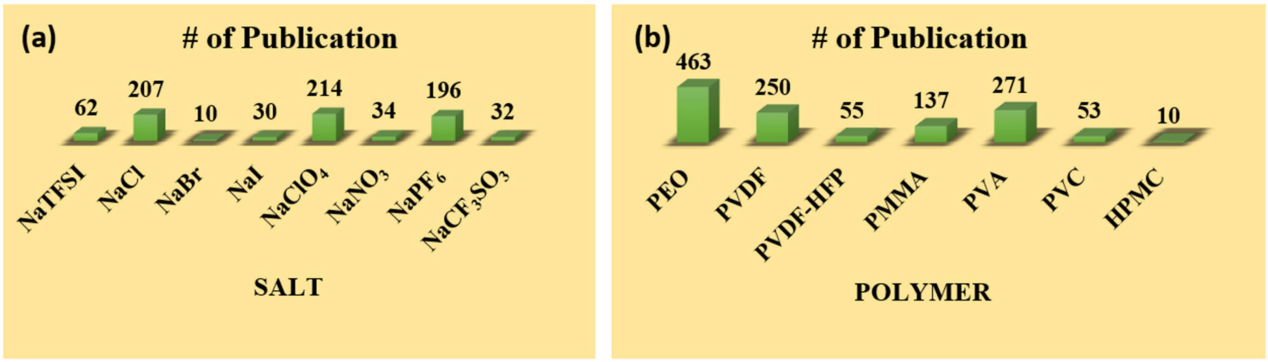

Figure 4. Advancements in sodium-ion battery research: (**a**) salt and (**b**) polymer.

This review aims to present a comprehensive overview of recent research advancements in PEs for SIBs. The focus is on relevant physical chemical properties, ionic conductivity, conduction mechanisms, and potential applications. We have critically examined challenges in PE research, proposing potential solutions. The discussion is articulated in three main sections: SPEs, GPEs, and CPEs. The primary objective is not only to provide a balanced assessment of the current state of the art of Na ion-conducting PEs but also to offer guidance for designing superior PEs as a critical component of SIBs. Additionally, future perspectives in the field are provided, anticipating the expected developments of PEs for next-generation SIBs.

2. Polymer Electrolytes

In order to overcome safety concerns negatively affecting Li-based batteries and enable high-energy-density electrical devices, the use of PEs in place of conventional liquid electrolytes has been recognized as the best way forward [30]. Research and development efforts have extensively delved into the synthesis, analysis, and utilization of PEs. Alkali metal salts dissolved in PEO were the first examples of conductive electrolytic complexes known as PEs, as Wright et al. demonstrated in 1973 [31]. In 1978, Armand et al. introduced an SPE consisting of PEO-Li salt for lithium-based batteries with an ionic conductivity of 10^{-4} S·cm^{-1} at 40–60 °C [32]. Another significant advancement took place in 1988 when Skaarup et al. demonstrated a conductivity of 10^{-3} S·cm^{-1} at ambient temperature [33]. PEs have drawn significant attention as potential substitutes to liquid electrolytes (Figure 5) because of their low flammability, processability, flexibility, and increased resilience to vibrational forces, stress, and mechanical deformation [34].

PEs surpass inorganic solid electrolytes in the context of electrode/electrolyte interfacial contact, and they outperform liquid electrolytes in terms of electrode/electrolyte compatibility. When compared to ceramics and glasses, polymers are typically more flexible and less expensive. Numerous polymers have been explored for their potential use in PEs, with examples including PEO, poly(methyl methacrylate) (PMMA), poly(vinylidene fluoride) (PVDF), poly(vinylidene fluoride hexafluoro propylene) (PVDF-HFP), and various others. Among these polymers, PEO-based materials have received the most intense research attention. This interest is due to the ability of the CH_2CH_2O units within the PEO chain to effectively solvate cations such as Li^+ and Na^+, as well as the high mobility of the polymer chain segments within PEO [35]. Similar benefits are provided by poly(ethylene glycol) or PEG, an α,ω-terminated PEO (Figure 6) [15]. Despite the superior electrochemical properties of PEs, their battery performance parameters such as long-term cycle stability can scarcely satisfy the demands in the practical application of LIBs and SIBs.

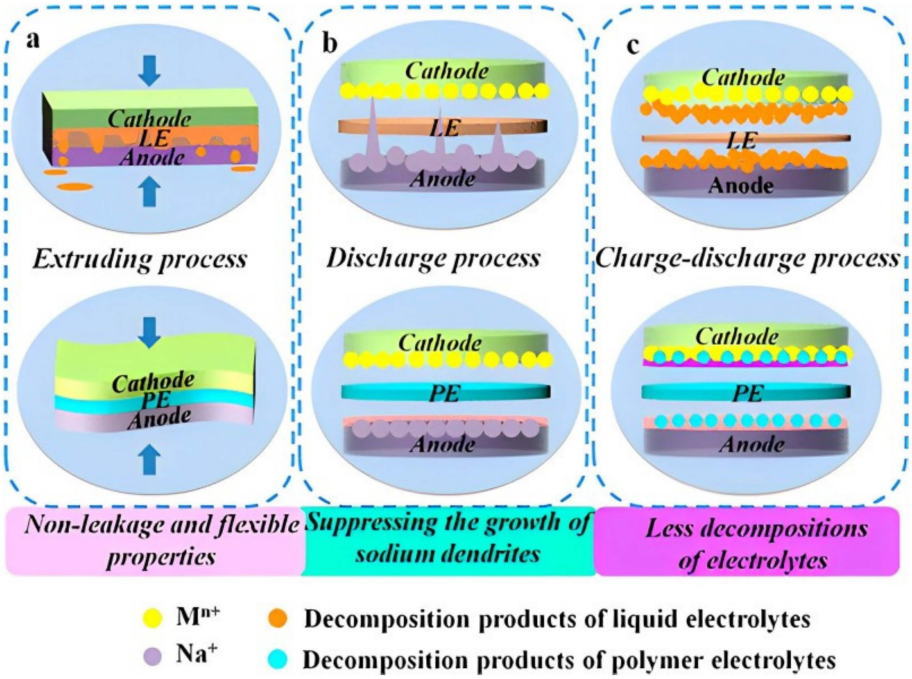

Figure 5. Comparison between liquid electrolytes and polymer electrolytes as they pertain to SIBs. Reprint with permission [15]; Copyright 2019, American Chemical Society.

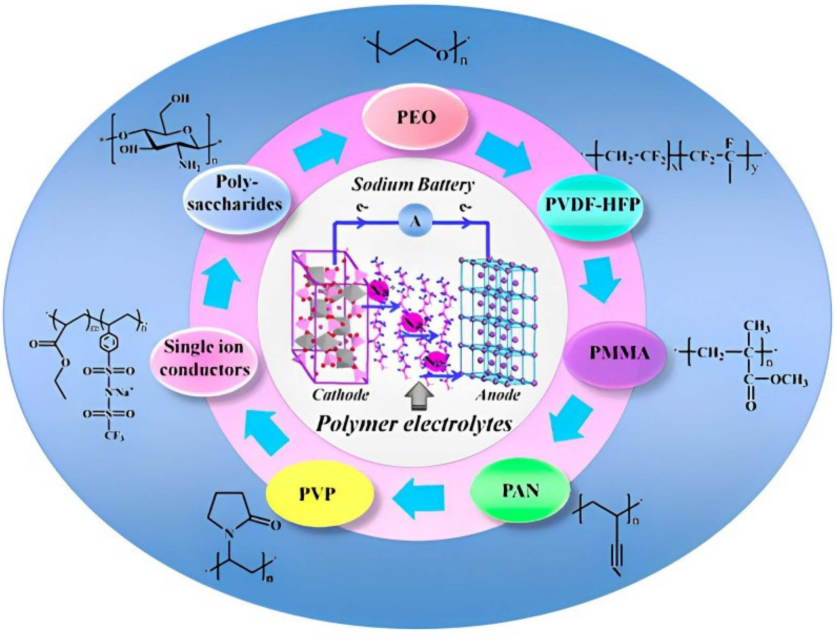

Figure 6. Polymer electrolytes for sodium batteries. Reprint with permission [15]; Copyright 2019, American Chemical Society.

Three main categories are considered when classifying PEs used in SIBs. The first type includes SPEs, in which only sodium salts ($NaPF_6$, $NaBF_4$, $NaClO_4$, etc.) are dissolved in polymer matrices [36,37]. The second type is represented by gel PEs (GPEs), which more stably combine solid and liquid phases. A liquid phase is trapped and swells into a polymeric network, thereby increasing the ionic conductivity of the polymeric phase and providing new conduction pathways [38,39]. The third type of PE is comprised of composite PEs (CPEs) [40]. We prefer to reserve the label of CPE for SPEs mixed with inorganic fillers [41,42]. Broadly speaking, a composite material is comprised of two or

more constituent materials, regardless of their nature. The introduction of additives in SPEs, whether organic or inorganic, technically still falls under the same definition. Unlike some authors, and in agreement with historical practice in the field, we prefer to refer to SPEs mixed with organic liquids as plasticized PEs (PPEs). Herein, this category is not discussed separately, but is considered only in conjunction with the main PEs. The principal reason for this choice is that few studies have been conducted in the direction of Na PPEs per se. Another category of PEs that will not be discussed in isolation is that of polymer ionic liquid electrolytes (PILEs), consisting of PEs mixed in with ionic liquids (ILs). The presence of inorganic fillers in CPEs imparts enhanced mechanical, thermal, and chemical stability while dramatically improving conductivity [43].

The ideal Na PE would be a solvent-free ion-conducting material with a conductivity above 10^{-3} S·cm^{-1} at room temperature, a cation transport number close to unity, and fire-retardant characteristics. The anion would bear a delocalized charge and would interact tightly with the polymer host without adversely affecting the electrodes. The compatibility of the PE with the electrode materials would also be important to assure the formation of a stable SEI on the anodic surface and a stable cathode–electrolyte interphase (CEI) on the cathodic surface. Incidentally, the fact that the CEI is much less studied than the SEI has been the likely source of undetected failure mechanisms in PEs and should be a more vigorous area of study for future improvements. The redox stability window of the ideal PE would be above 4 V, as enabled by the choice of non-labile terminal groups of the polymer host. It would also exhibit a solid consistency which renders the need for a separator superfluous and prevents or suppresses the formation of anodic dendrites. The ideal PE would be flexible and mechanically stable. It would also be thermally stable, with a low and fairly constant activation energy in a wide temperature range. It would exhibit a low glass transition temperature that would enable the assembly of reliable SIBs in cold climates. The addition of inorganic fillers would result in a higher conductivity but would also introduce disadvantages such as more difficult processing. It should be stated that even when envisioning the ideal Na PE, one needs to consider that, unfortunately, some of the desirable properties have proven thus far to be mutually exclusive.

Hereafter, we separately cover Na ion-conducting SPEs, GPEs, and CPEs. As shown below, some degree of overlap exists amongst these categories.

2.1. Solid Polymers Electrolytes (SPEs)

SPEs have garnered significant attention owing to their appealing properties, including their ease of transformation into thin films, good mechanical behavior, electrochemical stability, well-defined electrode/electrolyte interface, safety, and no leakage [44]. These characteristics are in stark contrast with those of liquid electrolytes. Notably, the concern towards the safety of lithium-based rechargeable batteries is related to the use of flammable liquid electrolytes. Although the lithium ion transference number is low for liquid electrolytes, they are endowed with a higher ionic conductivity and assure an appreciable interfacial contact with the electrode materials. However, there are disadvantages in addition to potential leakage, such as electrode/electrolyte reactions, which leads to an increase in battery temperature with consequent generation of flammable and hazardous gases [45–47]. Enhanced mechanical stability is imparted by the polymer backbone, and this characteristic is especially required for batteries in wearable devices [48]. SPEs are widely used in the fields of sensors and electrochemical energy storage devices such as batteries and supercapacitors, fuel cells, and electrochromic displays [12,49–51].

SPEs have garnered extensive research attention due to their combination of a relatively high ionic conductivity, cost-effectiveness, and mechanical stability [52]. In 1995, Hashmi et al. [53] investigated PEs based on PEO and $NaPF_6$ sandwiched between Pt electrodes. This PE system exhibited the best conductivity of 5×10^{-6} S·cm^{-1} at room temperature. In 1999, Sreekanth et al. [54] reported a PEO and $NaNO_3$ PEs measured between Na electrodes. Alternatively, the cathode was chosen to be a mixture of molecular iodine, carbon, and PE. The discharge characteristics were recorded at a constant load of 100 kΩ, and the

conductivity of the PEs was as high as 2.83 × 10^{-6} S·cm^{-1}. In 2001, Chandrasekaran et al. [55] reported a PE based on PEO and $NaClO_3$ with PEG, Na, and MnO_2 as the plasticizer, anode, and cathode, respectively. The authors concluded that the plasticizer activated the polymer chain relaxations, favoring an ion hopping mechanism within the polymer matrix. A higher conductivity value was observed with a lower salt concentration, measured at 9.47 × 10^{-4} S·cm^{-1}.

In 2005, Anantha et al. [52] reported studies of PEO-$NaNO_3$ PEs with different compositions of the ether oxygen to sodium ratio (O/Na). These PEs were formed into thin films using the solution casting method. Based on characterization studies, it was found that a decrement in crystallinity occurs with increasing salt concentrations. The highest conductivity of 3.5 × 10^{-6} S·cm^{-1} was observed at room temperature. In 2006, Kumar et al. [56] prepared a PE based on PEO and $NaClO_3$ using a solution casting technique and studied its properties in a cell with a Na anode, PE, and a mixture of I_2, with carbon and PE as the cathode. The PE was found to exhibit a conductivity value of approximately 10^{-7} S·cm^{-1}.

In the years 2006 and 2007, Mohan et al. [57,58] examined ion transport and battery discharge behavior in PEs derived from PEO and either $NaFeF_4$ or $NaLaF_4$. The optical and electrical properties were studied for pure PEO and PEO doped with the salts. Both the sodium compounds were prepared using a solid-state diffusion method by mixing NaF with $La(NO_3)_3$ and $Fe(NO_3)_3$, respectively. The conductivity of the PEs was shown to increase with rising temperatures using cells comprised of Na as the anode and a mixture of I_2 and C soaked with the electrolyte as the cathode. The maximum conductivity was found to be 1.37 × 10^{-7} S·cm^{-1} using $NaFeF_4$ and 3.9 × 10^{-7} S·cm^{-1} using $NaLaF_4$.

Consecutively, in the years 2006 and 2007, Bhide et al. [59,60] reported a new PE system using PEO, $NaPO_3$, and different ratios of ethylene oxide and $NaPO_3$ with and without PEG as a plasticizer. $NaPO_3$ was synthesized by gradually cooling the molten mixture of Na_2CO_3 and $(NH_4)H_2PO_4$ within the temperature range of 900 °C down to room temperature. This PE exhibited a peak conductivity of 2.8 × 10^{-8} S·cm^{-1}. Upon plasticization with PEG, the conductivity substantially increased to 8.9 × 10^{-7} S·cm^{-1}. In 2012, Sasikala et al. [61] reported their investigation of PEs composed of PEO and NaF. The conductivity demonstrated an upward trend with increasing NaF concentration, reaching a maximum value of 4.73 × 10^{-7} S·cm^{-1} at a PEO:NaF ratio of 70:30.

In 2017, Ma et al. [62] introduced a new PE incorporating sodium (fluorosulfonyl)(*n*-nonafluorobutanesulfonyl)imide (Na [(FSO_2)(*n*-$C4F_9SO_2$)N], NaFNFSI) and PEO. This PE exhibited a conductivity of 3.36 × 10^{-4} S·cm^{-1} at 80 °C. Another contribution was reported in the same year by Heratha et al. [63], who investigated the electrical and thermal characteristics of a PE system based on PEO and NaI, examining various PEO:NaI ratios. The highest conductivity recorded was 7.1 × 10^{-5} S·cm^{-1} at room temperature.

In 2019, Arya et al. [64] reported PEs based on PEO and $NaPF_6$ and studied their structural, morphological, electrochemical, and dielectric properties. These PEs, plasticized by succinonitrile, were found to exhibit a maximum conductivity of 2 × 10^{-5} S·cm^{-1}. The same authors reported on PEs comprised of a blended mixture of PEO, PVP, and $NaNO_3$ [65]. Their study centered on the dielectric relaxations and transport characteristics of this innovative polymer blend. A peak conductivity of 2.90 × 10^{-4} S·cm^{-1} at a temperature of 100 °C was observed. Again, in 2020, they reported a Na ion-conducting PE system based on a PEO and polyethyleneimine (PEI), which exhibited a conductivity of 5.2 × 10^{-4} S·cm^{-1} at 100 °C [66]. In 2020, Zhang et al. [67] reported on a PEO-$NaPF_6$ PE which exhibited a conductivity of 6.3 × 10^{-4} S·cm^{-1} at 80 °C. In that same year, Youcef et al. [68] reported on PEs based on PEO and a Na(FSI-ethyl cellulose) system which exhibited good electrochemical and mechanical properties, with a conductivity value of approximately 10^{-4} S·cm^{-1} at 80 °C.

In 2022, Kim et al. [69] published their findings regarding an anode-less seawater battery. This innovative battery utilizes an SPE based on a PEO polymer, facilitating energy storage from power to metal and metal to power. The precursors NaFSI, PEO, and Pyr_{14}FSI

were dried at 70 °C, 50 °C, and 90 °C, respectively, in a dry room for 24 h, followed by dissolution of benzophenone (a cross-linking agent) in $Pyr_{14}FSI$ to form a homogeneous solution. This mixture was added to PEO/NaFSI powder, mixed, sealed, and aged at 100 °C overnight. This material was then pressed into a thin polymeric film at 100 °C and treated with UV light. A peak conductivity of 1×10^{-3} S·cm^{-1} was recorded at room temperature. The SPE was integrated with a Na superionic conductor (NASICON) to achieve effective physical separation.

Chandra et al. [70] reported on their study of a PE based on PEO and NaCl with a ratio of 70:30. A peak conductivity of 4.5×10^{-6} S·cm^{-1} was recorded at room temperature. In 2006, Reddy et al. [71] studied the conductivity and discharge characteristics of a PE system based on PVC and $NaClO_4$. A viable solid-state electrochemical cell with a Na anode, the highest-conductivity PE, and a mixture of I_2, carbon, and PE as the cathode was fabricated. In 2017, Muhammad et al. [72] reported the properties of a PE based on PVC and NaI. The conductivity was 2.9×10^{-8} S·cm^{-1} at room temperature.

In 2006 and 2007, Bhargav et al. [73,74] reported on PE films based on PVA doped with NaBr and NaI salts. They studied the characteristics of PVA films with or without NaI or NaBr. It was found that as the concentration of the salts was increased, the films became more amorphous and, therefore, more conductive. Electrochemical cells were assembled using these electrolytes and characterized. The maximum conductivities obtained were 1.02×10^{-5} S·cm^{-1} and 1.12×10^{-6} S·cm^{-1} for NaI and NaBr, respectively. In 2018, Duraikkan et al. [75] studied the structural, thermal, and electrical properties of PEs comprised of PVA/PVP and $NaNO_3$. Similar to previous works, the amorphicity was found to increase, which in turn resulted in an increase of the conductivity to 1.25×10^{-5} S·cm^{-1} at room temperature. In 2021, Aziz et al. [76] reported on their study of a PE blend based on PVA and NaI using glycerol as a plasticizer, which was found to exhibit a maximum conductivity of 1.17×10^{-3} S·cm^{-1} at room temperature.

In 2013, Tiwari et al. [44] reported on starch-based sodium PEs. Potato starch was mixed with NaI, NaSCN, and $NaClO_4$ salts, and the effects of different anions were studied. The highest conductivity was measured for NaSCN at 1.12×10^{-4} S·cm^{-1}. In 2015, Khanmirzaei et al. [77] reported a PE based on the ionic liquid 1-methyl-3-propylimidazolium iodide (MPII) and rice starch (RS) for use in dye-sensitized solar cells. TiO_2 was coated on a fluoride/tin oxide (FTO) sheet and used as the anode, whereas platinum-coated FTO was used as the cathode, with RS:NaI:MPII as the electrolyte. This system was found to exhibit a peak conductivity at 1.20×10^{-3} S·cm^{-1}. In 2017, Ahmad et al. [78] carried out an electrical analysis of PEs based on cornstarch (CS) and NaCl. This simple PE exhibited the highest conductivity at 1.72×10^{-5} S·cm^{-1} for a weight ratio of 70:30 for CS:NaCl. In 2021, Awang et al. [79] studied the impact of adding sodium bisulfite, $NaHSO_3$, to cornstarch. The maximum observed conductivity was 2.22×10^{-4} S·cm^{-1} at room temperature. Similarly, in the same year, Asnawi et al. [80] reported the effects of adding $NaCF_3SO_3$ to a chitosan/dextran polymer blend. The resulting PE was found to exhibit a maximum conductivity of 6.10×10^{-5} S·cm^{-1} at room temperature.

In 2014, Rani et al. [81] conducted a comprehensive examination of the structural, thermal, and electrical attributes of PEs derived from hydroxypropyl methylcellulose (HPMC) doped with NaI. The best conductivity was recorded for the ratio of 5:4 for HPMC:NaI at 40 °C as 1.126×10^{-6} S·cm^{-1}. An enhanced amorphicity was accompanied by a high conductivity. In 2015, Abiddin et al. [82] reported on the conductivity and electrical properties of methylcellulose (MC) salted with NaI. The maximum conductivity that was observed was 2.7×10^{-5} S·cm^{-1} at 60 °C. Again, in 2015, Bella et al. [13] reported on the fabrication of a photo-PE based on a sodium ion methacrylate for secondary battery applications. This was the first report for a photopolymerized sodium ion PE. This material was found to exhibit a thermal stability greater than 100 °C, a high specific capacity, excellent chemical stability, and a high conductivity of 5.1×10^{-3} S·cm^{-1} at 20 °C. In 2020, Sayed et al. [83] studied the influence of different metal acetates on carboxy methylcellulose (CMC) in CMC-Na/PVP PEs by comparing their spectroscopic, optical, and dielectric

properties. Initially, the metal acetates of interest were added to PVP and then mixed with CMC-Na to form the PEs. The maximum conductivity was measured at 1.81×10^{-4} S·cm^{-1}. In 2020, Shetty et al. [84] conducted a study investigating the electrical and optical properties of CMC mixed with NaBr at various mass ratios. The highest conductivity, reaching 5.15×10^{-4} S·cm^{-1}, was achieved for the PE containing 20 wt% NaBr at room temperature. Similarly, Aziz et al. [46] reported a similar PE based on methyl cellulose (MC) doped with NaI, which demonstrated a maximum conductivity of 3.01×10^{-3} S·cm^{-1} with 50 wt% NaI.

In 2016, Singh et al. [85] reported PILEs based on an ionic liquid, 1-butyl-3-methyl imidazolium methylsulfate (BMIM-MS), PEO, and sodium methylsulfate salt. Various weight percentages of BMIM-MS were employed to formulate these electrolytes, which exhibited a maximum conductivity of 4×10^{-4} S·cm^{-1} at 75 ºC. In 2017, Zhang et al. [86] described the in situ formation of a PEG–divinyl ether PE. This ionic conductor was examined as a film on a polysulfonamide support alongside an $Na_3V_2(PO_4)_3$ cathode and a layered MoS_2 anode. The polymer, tri(ethylene glycol) divinyl ether, was polymerized in situ using $LiBF_4$ as an initiator, achieving a maximum conductivity of 1.2×10^{-3} S·cm^{-1} at ambient temperature. In 2017, Pan et al. [87] reported an SIB utilizing a single ion-conducting sodium ion PE composed of poly(*bis*(4-carbonyl benzene sulfonyl)imide-co-2,5-diamino benzesulfonic acid) (NaPA). The highest conductivity recorded for this system was 4.1×10^{-4} S·cm^{-1} at 80 °C. The cathodic material, $Na_3V_2(PO_4)_3$/AC was synthesized from the precursors H_3PO_4, NH_4VO_3, Na_2CO_3, and acetylene black. In 2018, Chen et al. [88] introduced a PE based on hyperbranched β-cyclodextrin (H-β-CD). The β-CD was modified using multiple oligo(methyl methacrylate)-block-oligo(ethylene glycol) methyl ether methacrylate short chains and complexed with NaTFSI, resulting in a self-standing, transparent, and flexible SPE film. This electrolyte exhibited its highest conductivity of 1.3×10^{-4} S·cm^{-1} at 60 °C. In the same year, Hassan et al. [50] investigated the structural and electrical spectroscopy of a PE composed of sodium 4-styrenesulfonate combined with ammonium nitrate. This PE displayed its highest conductivity at room temperature, reaching 3.16×10^{-4} S·cm^{-1} with a 30 wt% ammonium nitrate content.

In 2019, Janakiraman et al. [89] reported an electrospun fibrous PE based on PVDF combined with $NaPF_6$ for battery applications. In this technique, different concentrations of PVDF dissolved in DMSO and acetone were loaded into hypodermic syringes and were then subjected to electrospinning under an applied DC voltage. The resulting electrospun fibers were then soaked in an $NaPF_6$ solution and stretched for further analysis. This fibrous electrospun PE provided a maximum conductivity of 1.08×10^{-3} S·cm^{-1} at ambient temperature. In 2019, Yang et al. [90] reported a flame-retardant quasi-solid PE for battery applications. Poly(methyl vinyl ether-*alt*-maleic anhydride) (P(MVE-*alt*-MA), bacterial cellulose, and triethyl phosphate/vinylene carbonate (TEP/VC)/sodium perchlorate ($NaClO_4$) were used as the host, reinforcement, plasticizer, and salt, respectively. This PE was found to exhibit a flame-retardant nature and longer cycle stability. This system had a maximum conductivity of 2.2×10^{-4} S·cm^{-1} at room temperature. In 2021, Liu et al. [91] reported the synthesis of a single ion-conducting PE based on sodium *bis*(fluoroallyl)malonato borate salt NaBFMB photocrosslinked to a tri-thiol(trimethylolpropane tris(3-mercapto propionate) (TMPT) using a click thiol-ene reaction. This electrolyte exhibited a maximum conductivity value of 2×10^{-3} S·cm^{-1} at 30 °C. It is unclear to what extent the ILs were purely part of the 3D structure and whether there was some plasticizing effect due to the non-crosslinked IL.

In 2022, Law et al. [92] reported a hybrid dual-salt sodium PE for SIB applications. NaTFSI and NaDFOB salts were mixed together, followed by the addition of PVDF powder to form a blended SPE. This electrolyte was found to exhibit a maximum conductivity of 3.1×10^{-4} S·cm^{-1} at 23 °C.

Cisneros et al. proposed solvent-free sodium polymer batteries based on cross-linked PEs [93]. These electrolytes are formed through the polycondensation of α, ω-dihydroxy-oligo(oxyethylene) with an unsaturated dihalide, resulting in the formation of amorphous

networked electrolyte films upon further curing. Utilizing $NaClO_4$ and $NaCF_3SO_3$ at varying O/Na ratios, the optimal PE exhibits cationic conductivity (σ_+) surpassing 1 mS·cm^{-1} at 90 °C while maintaining mechanical integrity up to at least 120 °C.

Martínez et al. explored blends of PEO and poly(sodium 1-[3-(methacryloyloxy) propylsulfonyl]-1-(trifluoromethanesulfonyl) imide) (PNaMTFSI) in various proportions [94]. The blend composition significantly influenced the ionic conductivity, with the most notable results observed for blends containing 15 and 30 wt% PNaMTFSI. At elevated temperatures, specifically 85 °C, the highest ionic conductivity values were recorded, reaching 5.84×10^{-5} and 7.74×10^{-5} S·cm^{-1}, respectively. Furthermore, these compositions exhibited sodium ion transference numbers exceeding 0.83 and demonstrated electrochemical stability within the range of 3.5 to 4.5 V versus Na/Na$^+$. These findings suggest the potential use of these blends in sodium batteries.

The Na PEs explored thus far have been mostly based on PEO. Therefore, ethereal oxygens in a helical conformation appear to be the most reliable way to loosely coordinate and mobilize cations, including Na$^+$. Unfortunately, PEO, while enabling a relatively high conductivity (~10^{-4} S·cm^{-1}), is typically associated with a low transport number (below 0.5). An interesting alternative choice in polymer host has been that of cellulose derivatives, which provide the opportunity for using materials of biological origin. It remains unclear to what extent OH-rich phases can be fully dried of water traces and become thermally stable upon prologued cycling. At the same time, the knowledge transfer of Li to Na as it pertains to salts (e.g., $NaPF_6$, NaTFSI, and NaFSI) did not present any particular surprises or improvements. Based on general cation solubility principles, it is doubtful that further fine tuning may come from structural modifications of already available anions.

2.2. Gel Polymers Electrolytes (GPEs)

GPEs have gained significant importance due to their ability to combine the advantageous characteristics of both solid and liquid electrolytes [95]. Feuillade et al. [96] conducted pioneering research on GPEs for Li batteries in 1975, the first of such studies on record. In their work, they explored cross-linked gel membranes composed of materials like polyvinyl butyral (PVB), epichlorohydrin with titanium/silicon alkoxy compounds, PVDF and dicinnamylidene hexanediamine dissolved in methyl ethyl ketone. Additionally, they investigated thermoplastic gels consisting of PAN, PC, and NH_4ClO_4. GPEs are produced by over-plasticizing the polymeric phase with low-molecular-weight molecules, usually organic solvents. As a result of its interaction with the plasticizer, the polymer expands and mostly becomes amorphous while maintaining adequate mechanical strength. The plasticizer's presence enables new avenues for ionic movement. These reasons explain why SPEs without plasticizers often have lower conductivities than GPEs [97,98]. The precise ion-conduction mechanism and the nature of the interactions between the polymer, plasticizer (solvent), and salt have yet to be fully elucidated [99,100]. GPEs have recently attracted attention due to their superior characteristics over liquid electrolytes [101]. Their most attractive quality is their free-standing consistency, which facilitates handling, cell design, modularity, and dependability in many electrochemical devices [102].

In order to enable the functionality of GPEs, it is necessary to incorporate plasticizers or solvents possessing elevated dielectric constants. These are blended with different salts and fixed within the structure of polymer matrices, including materials such as PMMA, PAN, PVDF, and PVDF-HFP, among others [103–106]. GPEs can develop when appropriate ionic salts and small-sized organic solvents like EC, PC, and DEC are enclosed within the polymer hosts [107]. The co-polymer PVDF-HFP is widely used in high-performance GPE systems among the many host polymers because of its advantageous properties such as its low glass transition temperature (−35 °C), high dielectric constant (8.4), and structural uniqueness. GPEs have a strong ionic conductivity, exhibit increased safety, are inexpensive, and are simple to fabricate into the desired shapes and sizes. The thermal, mechanical, chemical, and electrochemical stability of GPEs are adequate. Further improvements in

GPEs would require electrolyte salts with a superior solubility and high liquid holding capacity.

Room-temperature ionic liquids (RTILs) have been employed as substitutes for organic additives in GPEs to enhance their thermal, mechanical, and electrochemical durability. ILs are molten salts composed primarily of organic cations and inorganic anions. They are appreciated for their versatility and their effective roles as plasticizers and suitable solvents. Their distinctive attributes include their robust ionic conductivity (0.01 $S{\cdot}cm^{-1}$), elevated thermal stability up to 400–500 °C, non-flammability, non-volatility, and impressive electrochemical window spanning the range of 4.0–6.0 V [108].

Wang et al. [109] assembled Na-conducting GPE membranes using $Na_2Zn_2TeO_6$ as a filler, and their use in SIBs was shown to be effective. The incorporation of $Na_2Zn_2TeO_6$ filler led to a composite GPE (CGPE), with a substantial enhancement in ionic conductivity. This improvement can be attributed to the filler, which also functions as an ionic conductor, causing a reduction in the crystalline structure and an increase in the porosity within the polymer membranes. Consequently, the modified GPE membranes exhibit an impressive ionic conductivity of 2.52 $\times$ 10^{-3} $S{\cdot}cm^{-1}$ at room temperature, along with an extremely low activation energy of approximately 0.040 eV. The assembled $Na_3V_2(PO_4)_3$/C | GPE | Na battery showcases excellent performance metrics, including a notable initial discharge capacity of 93.3 $mAh{\cdot}g^{-1}$ at 0.5 C, a promising capacity retention rate of 98.4% after 100 cycles, and outstanding high-rate performance, achieving 83.5 $mAh{\cdot}g^{-1}$ at 5 C.

This research establishes that ionic conductors such as $Na_2Zn_2TeO_6$ can be used to improve GPE performance. Using a conventional solid-state reaction approach carried out using high-energy ball milling, $Na_2Zn_2TeO_6$ filler was produced. PVDF-HFP/PMMA-based GPEs membranes with $Na_2Zn_2TeO_6$ were prepared using the solution casting process. X-ray diffraction was employed to examine the phase structure of the as-prepared $Na_2Zn_2TeO_6$ filler and the filer within the GPE membranes. Field emission scanning electron microscopy was used to analyze the microstructure and elemental distribution of the GPE membranes. Thermogravimetric analyses were performed from room temperature to 700 °C.

Wang et al. [110] synthesized a new polymeric material termed polymeric sodium tartaric acid borate (PSTB), which was combined with poly(vinylene carbonate) to produce a single-ion-conducting GPE referred to as PSP-GPE. This PSP-GPE exhibited several notable characteristics, including a high sodium ion transference number of 0.88, an oxidation threshold of 4.5 V, and excellent compatibility with the sodium anode. Furthermore, it showed remarkable ionic conductivity, registering at 1 $\times$ 10^{-4} $S{\cdot}cm^{-1}$, surpassing the performance of a room-temperature liquid electrolyte based on $NaClO_4$. A Na/PSP-$_{10}$-GPE/$Na_3V_2(PO_4)_3$ battery was found to exhibit a 98.6% capacity retention and >99% coulombic efficiency for 200 cycles at 0.5 C, 25 °C. The same assembly at 60 °C exhibited an approximately 100% capacity retention and >99.3% coulombic efficiency for 50 cycles at 0.5 C.

Wang et al. [111] prepared a novel CGPE membrane by blending PVDF-HFP/PMMA with $Ti_3C_2T_x$ MXene. They then investigated the electrochemical performance of this membrane in SIBs. The presence of the $Ti_3C_2T_x$ MXene filler, which is multilayered, significantly enhanced the electrochemical performance of the battery. This improvement was attributed to the filler's ability to increase the contact sites for Na ions and enhance the porosity of the polymer membranes. Furthermore, the distinctive parallelly arranged layered structure of the MXene promoted uniform sodium nucleation and growth on the surface of the sodium electrode while inhibiting the formation of sodium dendrites during the sodium deposition process. The CGPE membrane containing 8 wt% $Ti_3C_2T_x$ MXene exhibited impressive properties, including a maximum ionic conductivity of 3.28 $\times$ 10^{-3} $S{\cdot}cm^{-1}$, excellent thermal stability, a relatively high sodium ion transfer number of 0.558, and a wide electrochemical window of 5.25 V. A $Na_3V_2(PO_4)_3$/GPE/Na battery after 300 room temperature cycles at 0.5 C showed a remarkable 95% capacity retention. The $Na_3V_2(PO_4)_3$ cathode was prepared using a sol-gel process [45].

To achieve good sodium ion conductivity at room temperature, Vo et al. [112] prepared GPE films employing a PVDF-HFP matrix. Microporous PVDF-HFP membranes were swelled and filled with various liquid electrolytes comprised of $NaClO_4$, $NaPF_6$, and NaTFSI salts dissolved in mixtures of carbonate solvents such as PC and fluoroethylene carbonate (FEC) or ionic liquids such as 1-ethyl-3-methylimidazolium *bis*(trifluoromethane). The influences of the different electrolytes on the structure, morphology, electrolyte absorption, and sodium ionic conductivity of the resulting membranes were examined by the authors. The "sponge-like" structure of the GPEs was endowed with a high porosity (80–85%) and large pore sizes. At ambient temperature, the ionic conductivity of the GPEs was 1–2 $mS{\cdot}cm^{-1}$. DSC, TGA, XRD, and FE-SEM were used for characterization. By employing GPEs as the ion-conduction layer, sodium intercalation into an $Na_{0.44}MnO_2$ cathode was carried out in a coin-cell configuration. At room temperature, the cycling data of a sodium cell using PVDF-HFP/$NaClO_4$ 1 M-PC:2%FEC showed a consistent specific capacity of 100 $mAh{\cdot}g^{-1}$. The best ionic conductivity was 1.91 $mS{\cdot}cm^{-1}$ for $NaClO_4$ 1 M PC:2%FEC/PVDF-HFP. The temperature-dependent ionic conductivity exhibited VTF behavior, indicating the assistance of the backbone and polymer segmental mobility in the gel medium. The higher temperature of liquid electrolyte degradation when compared to the unsolvated microfiber membrane imparted a higher thermal stability to the final GPEs. Due to the high oxidation limit of 4 V ca. vs. the Na^+/Na potential, the electrochemical stability window of the GPEs was compatible with 4 V sodium cathode materials. The assembly of a Na/GPE/$Na_{0.44}MnO_2$ cell allowed the authors to demonstrate a reversible intercalation/deintercalation of Na^+, as well as a steady discharge capacity in a cyclic voltammogram and charge–discharge test. After 20 cycles, the specific capacity of $NaClO_4$ 1 M—PC:2%FEC/PVDF-HFP remained constant at 100 $mAh.g^{-1}$, with no sign of capacity fading.

Harshlata et al. [113] demonstrated that a liquid electrolyte composed of sodium trifluoromethanesulfonate ($NaCF_3SO_3$) dispersed within an IL named 1-butyl-3-methylimidazolium trifluoromethanesulfonate ($BMImCF_3SO_3$) can be effectively immobilized using a porous membrane crafted from PVDF-HFP. The manufacturing process for these porous GPE membranes involved a phase-inversion technique. Various physical and electrochemical methods were utilized to characterize these electrolyte membranes. Notably, in the CGPE systems, the incorporation of TiO_2 nanoparticles led to interactions with the anion of the liquid electrolyte ($CF_3SO_3{}^-$) and resulted in an increased amorphicity of the polymer network. As a result, the improved membrane exhibited enhanced electrochemical stability, with a window of approximately 4.3 V, a maximum room temperature ionic conductivity of 0.4 $mS{\cdot}cm^{-1}$, and a Na^+ ion transport number of roughly 0.27. This upgraded membrane was employed in the construction of a prototype sodium battery, which displayed a consistent open-circuit potential of 2.2 V and delivered a discharge capacity of 200 $mAh{\cdot}g^{-1}$ at a drain current of 25 $mAh{\cdot}g^{-1}$. To investigate the structural properties of the membrane, various characterization techniques were employed, including scanning electron microscopy (SEM), X-ray diffraction (XRD), and Fourier transform–infrared spectroscopy (FTIR).

Utilizing the highest-performing composite PILE membrane denoted as PEM0.5, a prototype sodium battery was assembled featuring a sodium–mercury (Na-Hg) anode and a phosphorus–carbon (P-C) cathode. When compared to pure sodium metal, Na-Hg serves as a superior reducing agent and is easier to handle. Phosphorus red, with a theoretical capacity of 2596 $mAh{\cdot}g^{-1}$, emerges as an excellent candidate for the electrode material in a sodium battery, while carbon contributes the electronic conductivity [10].

Chen et al. [114] synthesized a flexible GPE (PGT32-5%) based on poly(poly(ethylineglycol) methacrylate) (PPEGMA) that was plasticized with nonflammable triethyl phosphate (TEP). The GPE was then stabilized by glass fibers using an in situ thermal curing process. A high ionic conductivity (9.1×10^{-4} $S{\cdot}cm^{-1}$ at 27 °C) and wide electrochemical window are two characteristics of the improved flame-retardant electrolyte, PGT32-5% (4.8 V). To ensure excellent cycling stability of the quasi-solid-state $Na_3V_2(PO_4)_3$ | PGT32-5% | Na battery (capacity retention of 91% after 400 cycles), an artificial interface between the GPE and Na

metal anode was formed. It was found that trace FEC on a hard-carbon anode can generate a stable SEI [115]. Furthermore, the interfacial modification and its impact on the discharge behavior were thoroughly examined, paving the way for the development of future PEs that exhibit superior performance parameters. The sol-gel process was followed to produce the $Na_3V_2(PO_4)_3/C$ cathode [116].

Lonchakova et al. [117] prepared a highly effective polyacrylonitrile-based GPE for SIBs by using commercially available copolymer poly(acrylonitrile-co-methyl acrylate), propylene carbonate as a plasticizer, and either $NaClO_4$ or $NaPF_6$ as salts. These authors conducted AC impedance measurements, focusing on reversible rather than blocking electrodes, to determine the specific and molar conductivities at varying salt concentrations. The cation transference numbers were measured using the potentiostatic polarization method. The resulting electrolytes exhibited impressive ionic conductivities of up to 1.8×10^{-3} S·cm^{-1} at room temperature and high cation transference numbers of up to 0.89. The conductivity displayed Arrhenius behavior, with an activation energy ranging from 12 to 15 kJ·mol^{-1}. In sodium ion cells operating at both room temperature and 20 °C, the GPE demonstrated an excellent stability, enduring over 700 charge–discharge cycles. These findings indicate that polyacrylonitrile-based GPEs hold promise as alternatives to liquid electrolytes in SIBs.

Tian et al. [118] synthesized a new fluorine-containing ionomer using PVDF and propylene glycol carbonate (PGC). The result was the discovery of remarkable single-ion-conducting GPEs. The cation–carbonyl interactions, morphology, and ion-conduction characteristics of the GPEs were investigated using NMR, DSC, SEM, and complex impedance analyses. The GPEs were found to consist of three phases: a liquid electrolyte phase, an amorphous swelling phase, and a polymer crystalline phase according to the DSC and SEM examinations. Both the FT-IR study and the NMR data revealed that sodium ions form bonds with carbonyl groups of vinyl acetate and perfluoro(5-methyl-3,6-dioxo-8-fluoride sulfonyl-1-octene). Both the amount of PGC and the amount of fluorine-containing ionomer had a significant impact on the morphology and ionic conductivity of the samples. This new GPE system showed an ionic conductivity above 10^{-4} S·cm^{-1} at ambient temperature, with a sodium ion transport number of more than 0.99 ($t_+ > 0.99$).

Parveen et al. [119] conducted a study focusing on the development of novel GPEs for battery applications. Their work centered on solvate ionic liquids (SILs), which featured complex cations [Na-(glyme)]$^+$ and ClO_4^- anions. To produce these SIL-GPEs, they adjusted the $NaClO_4$ content in triglyme (G3) and immobilized the resulting electrolyte within a PVDF-HFP matrix. The result was the formation of flexible, self-supporting films. A comprehensive range of analytical techniques, including SEM, XRD, FTIR, Raman spectroscopy, and thermal gravimetric (TG) analyses, were employed to investigate the morphology, structure, and interactions between the salt, glyme, and polymer in these materials. In their ideal composition, which consisted of a 0.3:1 molar ratio of $NaClO_4$ to G3, electrochemical assessments demonstrated outstanding characteristics, including a high ionic conductivity of approximately 2.54×10^{-3} S·cm^{-1}, a substantial Na ion transport number of approximately 0.73, and an extensive electrochemical stability window of 4.7 V.

The effectiveness of these SIL-GPEs was evaluated in a quasi-solid-state sodium ion battery by constructing a half-cell with a positive electrode composed of ball-milled V_2O_5. This battery exhibited a sustained capacity of approximately 55 mAh·g^{-1} after 65 charge-discharge cycles at 0.1 C, achieving a maximum capacity of 111 mAh·g^{-1} for the initial cycle at a current rate of 0.05 C. The active material for the electrodes was produced through a straightforward ball-milling procedure [120].

Kumar et al. [121] reported an innovative thermally and electrochemically stable sodium ion-conducting GPE including an ionic liquid at room temperature called 1-ethyl-3-methyl imidazolium trifluoro-methane sulfonate (EMI-triflate or EMITf) with sodium triflate ($NaCF_3SO_3$) as a salt, immobilized in PVDF-HFP. FTIR, SEM, and XRD were used to study the conformational and structural changes in PVDF-HFP caused by the entrapment of an EMImTf or EMImTf/NaTf solution. A total of 0.5 M of the electrolyte with the

formula EMImTf:PVdF-HFP (4:1 *w*/*w*) in the form of a free-standing thick film exhibited an ionic conductivity of 5.74 × 10^{-3} S·cm^{-1} at room temperature (∼27 °C), and NaTf showed exceptional dimensional stability. The ionic conductivity of the GPEs as a function of temperature was compatible with VTF behavior. The Na^+ ion transport number was found to be ∼0.23, indicating a large contribution from anionic transport as well as potential conduction of the component ions of the IL.

Kumar et al. [122] prepared flame-retardant GPEs based on trimethyl phosphate (TMP) for safer electrochemical applications utilizing the solution casting approach. XRD, DSC, EIS, and LSV were used to characterize these sodium ion-conducting materials. Physical investigations showed that the electrolyte using TMP solvent had a greater amorphicity and thermal stability compared to the binary mixture of ethylene carbonate (EC) and propylene carbonate (PC) that is commonly utilized. When compared to a membrane with an EC:PC solvent mixture, the TMP-based electrolyte membrane exhibited improved ionic conductivity (~1.40 mS·cm^{-1}), a wider electrochemical stability window of ~4.5 V, and superior Na^+ transport properties. The electrolyte based on TMP has been used in an electric double-layer capacitor (EDLC) and in prototype sodium batteries. The best Na battery has a specific discharge capacity of 225 mA·hg^{-1} and an open circuit voltage of ~2.3 V. The TMP-based electrolyte and activated carbon electrodes were used to produce an EDLC with a specific capacitance of ~100 F·g^{-1} that was stable for up to 4000 charge–discharge cycles.

Mishra et al. [123] introduced an ionic liquid (IL) into a PVDF-HFP matrix at a high loading level. To create GPE films with polar characteristics, various amounts of PVDF-HFP were blended with a 1 M solution of sodium *bis*(trifluoromethylsulfonyl)imide salt (S) in 1-butyl-3-methylimidazolium *bis*(trifluoromethylsulfonyl)imide IL to form what the authors called a salt–IL (SIL) solution. They employed a scaling technique and dielectric relaxation analysis to ascertain the temperature- and frequency-dependent ionic conductivities of these GPEs. The GPE containing 70 weight percent SIL (referred to as PSIL70) demonstrated outstanding thermal stability up to 368 °C, a high ionic conductivity of 1.9 × 10^{-3} S·cm^{-1}, and a sodium ion transference number of 0.27. Additionally, it exhibited a broad electrochemical stability window of 4.2 V versus Na/Na^+ at 30 °C. To construct a coin cell (Na/PSIL70/Na-NMC), they paired a Na–NMC cathode with a Na–metal anode using the optimized electrolyte PSIL70. The charge–discharge results showed that the cell had a specific discharge capacity of 108 mAh·g^{-1} at a rate of 0.1 C (equivalent to 21 mAh·g^{-1}). The sodium battery had a large capacity and a capacity retention of 94% after 200 cycles at 0.2 C.

The effects of mixing PMMA with PVDF-HFP and a non-aqueous liquid electrolyte of $NaCF_3SO_3$ in a binary mixture of EC and PC were reported by Mishra et al. [124]. Utilizing XRD, SEM, complex impedance spectroscopy, LSV, and determination of the ion transport number, it was shown how compositional changes in PMMA affect the GPE system. The improved electrolyte composition provided a sufficiently wide electrochemical stability window of 3.6 V. It was determined that the PVDF-HFP-based GPE had an ionic conductivity of ~6.1 × 10^{-4} S·cm^{-1} at room temperature. When PVDF-HFP and PMMA were combined, the ionic conductivity of the GPE was raised to ~7.5 × 10^{-4} S·cm^{-1} (9:1). The porous and predominately amorphous character of the GPEs upon polymer mixing was supported by SEM and XRD tests.

According to Chauhan et al. [125], sodium aluminate ($NaAlO_2$) active fillers that were dispersed in porous GPEs improved the electrochemical performance parameters. Phase inversion was used to synthesize microporous sodium ion-conducting GPE sheets. The filler particles in the resulting CGPE system improved the retention of the sodium salt solution, increasing the ionic conductivity from 0.22 mS·cm^{-1} to a maximum of 0.68 mS·cm^{-1} for an optimum composition of 0.50 wt% $NaAlO_2$. The improved compositions exhibited better electrochemical stabilities and Na^+ transference numbers than the unfilled GPE. Ion dynamics studies of the CGPE system, investigated via dielectric analysis, showed that the $NaAlO_2$ fillers introduced amorphicity into the polymer network. Ionic motion is

supported by the segmental motion of the polymer host and by the Na^+-AlO_2^- dipoles. The prototype Na-S battery based on the sample PGPE0.50 at RT exhibited a steady open circuit voltage of ~2.2 V. At drain currents of 0.10, 0.25, and 0.50 mA cm^{-2}, the cell showed discharge capacities of ~210, 139, and 51 $mAh{\cdot}g^{-1}$, respectively.

Janakiraman et al. [126] proposed a separator made from electrospun amorphous PVDF-HFP as a superior GPE material that is appropriate for sodium ion cells. To achieve an amorphous electroactive β-phase structure, a 16% polymer solution was electrospun at an 18 kV voltage. This electrospun material served as a separator membrane in a liquid electrolyte solution containing 0.6 M sodium hexafluorophosphate ($NaPF_6$) dissolved in a mixture of ethylene carbonate and propylene carbonate (EC:PC, 1:1, vol.%). The researchers conducted investigations into the ionic conductivity, electrolyte uptake, and linear sweep voltammetry (LSV) of this amorphous GPE. The GPE exhibited a wide electrochemical stability range, extending up to 4.6 V versus Na/Na^+ at room temperature, and displayed a high ionic conductivity of 1.28×10^{-3} $S{\cdot}cm^{-1}$. Furthermore, when applied to cells with the configuration $Na/GPE/Na_{0.66}Fe_{0.5}Mn_{0.5}O_2$, these cells demonstrated exceptional cycling performance with minimal capacity loss.

Janakiraman et al. [127] explored the use of an electrospun fibrous membrane made from amorphous P(VDF-co-HFP) for sodium ion battery applications. They employed techniques like X-ray diffraction (XRD), field emission scanning electron microscopy (FESEM), and atomic force microscopy (AFM) to examine the physical and chemical properties of the freshly produced fibrous polymer membranes. These fibrous membranes, produced in an argon-filled glove box, were combined with a liquid electrolyte solution containing 1 M $NaClO_4$ in a mixture of ethylene carbonate and diethyl carbonate (EC:DEC, 1:1 by volume). In contrast to the commercial Celgard membrane, the electrospun PVDF-HFP-based polymer membrane exhibited an extremely porous structure and boasted a high ionic conductivity of 1.13×10^{-3} $S{\cdot}cm^{-1}$. Furthermore, the electrochemical stability window of this separator-cum gel polymer electrolyte (SGPE) against Na^+/Na exceeded 4.8 V. The researchers also conducted electrochemical studies on a sodium half-cell where they used the SGPE as the separator, $NaNi_{0.5}Mn_{0.5}O_2$ as the cathode, and pure sodium as the anode. After 50 cycles at a 0.1 C rate, the cell displayed a columbic efficiency of 97%, albeit with some capacity loss over time.

The development of sodium metal batteries (SMBs) is hampered by the drawbacks of typical organic liquid electrolytes, such as sodium dendrite formation, harmful side effects, and liquid leakage. A novel sodium poly(tartaric acid)borate (NaPTAB) salt was successfully synthesized by Yang et al. [128] through an environmentally friendly and cost-effective method known as aqueous-phase synthesis. To synthesize a single sodium ion conductor GPE called NaPTAB-SGPE, NaPTAB was combined with PVDF-HFP to form NaPTAB-SM. NaPTAB-SGPE demonstrated an exceptional thermal stability, with an initial decomposition temperature of 345 °C. It exhibited a noteworthy ionic conductivity of up to 9.4×10^{-5} $S{\cdot}cm^{-1}$ at room temperature, a wide electrochemical stability window extending up to 5.2 V (vs. Na^+/Na) at 30 °C, and a high sodium ion transference number of 0.91 at 60 °C. Additionally, when incorporated into $Na_3V_2(PO_4)_3/Na$ cells, NaPTAB-SGPE displayed an outstanding charge–discharge performance and consistent cycling capabilities, even at elevated temperatures (60 °C). Notably, it exhibited improved cycle stability compared to liquid electrolyte cells containing 1 M $NaClO_4$ (EC:PC, 1:1, v/v, and 5% fluoroethylene carbonate (FEC)). The GPE membrane began to produce NaF after cycling, as seen using ^{23}Na and ^{19}F solid-state NMR. This phenomenon is more likely to be the cause of the observed remarkable charge–discharge stability and cycling performance of the battery. These findings indicate that NaPTAB-SGPE is a highly promising replacement for solid-state sodium batteries.

The use of a nonflammable electrolyte is important to overcome the safety concerns of SIBs. Due to their outstanding fire-extinguishing qualities, organic phosphorus compounds like phosphates and phosphonates have been actively investigated as flame-retardant additives [129,130]. Park et al. [131] report on ion-conductive polycaprolactone triacrylate-

containing gel precursors that were cross-linked in situ to produce nonflammable GPEs. Despite having a three-dimensional network structure, the GPEs have a high ionic conductivity of up to 6.3 $mS{\cdot}cm^{-1}$ due to the Na^+–carbonyl coordination and strong segmental mobility of polycaprolactone chains. By causing uniform Na deposition on the Na electrode, the ion-conductive polymer networks effectively inhibit the growth of Na dendrites, which improves the interfacial properties of the anode. The Na/GPE/$Na_3V_2(PO_4)_3$ cell shows remarkable cycle stability and offers high discharge capacities at high C rates. Additionally, these cells can operate safely because of the greater thermal stability of the GPE, which prevents short circuiting of the cell at high temperatures.

By using a self-catalyzed method, Niu et al. [132] prepared a novel GPE with a cross-linked polyether network (GPE-CPN). In situ copolymerization of two monomers, 1,3-dioxolane and trimethylolpropane triglycidyl ether, was successfully achieved with the use of sodium hexafluorophosphate ($NaPF_6$) as an initiator. The authors showed that the resulting GPE-CPN had an improved electrochemical stability window against Na^+/Na up to 4 V and a significant ionic conductivity of 8.2×10^{-4} $S{\cdot}cm^{-1}$ at room temperature. The electrolytes inhibited the growth of sodium dendrites and stabilized the electrolyte/sodium anode interface. The as-prepared GPE-CPN showed promise for future use in rechargeable SIBs when taking into account the advantages of its simple manufacturing and exceptional properties. $Na_3V_2(PO_4)_3$, $Na(Li_{0.05}Ni_{0.3}Mn_{0.5}Cu_{0.1}Mg_{0.05})O_2$, and $NaTi_2(PO_4)_3$ electrode materials were utilized in this study. The GPE system presented superior interfacial stability toward both the cathode and the anode in electrochemical tests.

Farhana et al. [133] prepared GPEs using a poly(propylene) carbonate (PPC) polymer and various weight percentages of sodium iodide (NaI) salt. The plasticizers included ethyl carbonate (EC) and propyl carbonate (PC). At room temperature, a maximum ionic conductivity of 2.01 $mS{\cdot}cm^{-1}$ was attained. The structural characteristics of the GPEs were investigated using FTIR. A complexation between PPC and NaI occurred based on the FTIR study. Dye-sensitized solar cells (DSSC) were produced utilizing GPEs under one sunlight intensity and subjected to photovoltaic investigations. The greatest energy conversion efficiency of 6.38% was attained with the incorporation of 60 wt% of NaI. The ionic conductivity was indeed improved by adding NaI salt to PPC:EC:PC. The highest ionic conductivity was 2.01 $mS{\cdot}cm^{-1}$ with an activation energy of 0.150 eV, as predicted by the Arrhenius model.

Jyothi et al. [134] synthesized polyacrylonitrile (PAN)-based sodium ion-conducting GPEs using EC and DMF as plasticizing solvents using a solution casting technique. These GPEs were translucent, dimensionally stable, free-standing films. NaI was the source of Na^+ ions. The conductivity changes were studied as a function of salt concentration from 10 to 40 weight percent. The sample with 30 weight percent of NaI had the maximum conductivity, measuring 2.35×10^{-4} $S{\cdot}cm^{-1}$ at 303 K and 19×10^{-3} $S{\cdot}cm^{-1}$ at 373 K. With an activation energy in the region of 0.25 to 0.46 eV, the conductivity–temperature dependence of the PE sheets obeyed the Arrhenius equation. Using Wagner's polarization approach, the transport numbers, both electronic (t_e) and ionic (t_i), were measured. It was revealed that the conducting species were predominantly due to ions. The highest cationic transport number was determined to be 0.991. The best conducting GPE system was used in the development of a solid-state battery with the configuration Na/(PAN/NaI)/(I_2/C/GPE), and the discharge characteristics of the cell were assessed against a load of 100 kOhm. The Na^+ ions were more mobile and contributed to cation conductivity because, according to the FT-IR spectra, they were situated adjacent to the C=O groups of the plasticizers and the C:N groups of PAN with only minor electrostatic contacts. According to the DSC thermograms, the addition of the plasticizing solvents EC and DMF made the PE more amorphous, whereas the addition of NaI salt made it stronger. As the NaI concentration rose, the conductivity rose as well, which was ascribed to an increase in amorphicity. The increase in conductivity with rising temperatures was attributed to ion hopping. It was recognized that as the ionic conductivity and dopant concentration increased, the activation energy decreased.

Zhang et al. [135] prepared a GPE by enclosing an improved Na^+/Zn^{2+} mixed-ion aqueous electrolyte in a polyacrylonitrile nanofiber polymer matrix. An innovative aqueous sodium ion battery (ASIB) system was constructed by employing this electrolyte, a zinc anode, and a $Na_4Mn_9O_{18}$ cathode. $Na_4Mn_9O_{18}$, which resembles nanorods, was synthesized via a hydrothermal soft chemical reaction. The distribution of the crystalline $Na_4Mn_9O_{18}$ nanorods on the cathode was validated via structural and morphological measurements. The Zn/GPE/$Na_4Mn_9O_{18}$ battery exhibited excellent cycle stability at a good performance rate, as established by electrochemical experiments. The battery was characterized by an initial discharge capacity of 96 mAh·g^{-1} and a 64 mAh·g^{-1} capacity after 200 cycles at a 1 C cycling rate. The Zn/GPE/$Na_4Mn_9O_{18}$ battery is a promising and safe high-performance battery. Using a hydrothermal soft chemical reaction (HSCR), $Na_4Mn_9O_{18}$ nanorods were successfully produced.

A sodium superionic conductor (NASICON) with the formula $Na_3Sc_2P_3O_{12}$ (NSP) exists in three crystalline phases, namely α-, β-, and γ. Its ion transport characteristics and other electrochemical properties depend on the crystal phase. Mei et al. [136] conducted a thorough investigation of the impacts of crystalline NASICON fillers with different stoichiometries, such as $Na_3Sc_2P_3O_{12}$, $Na_{3.5}Sc_2P_{2.5}Si_{0.5}O_{12}$, and $Na_4Sc_2P_2SiO_{12}$, on GPEs based on PVDF-HFP/PMMA. The three fillers had different adsorption capacities, and this resulted in a range of performances for the resulting CGPEs. At 64 °C and 166 °C, $Na_3Sc_2P_3O_{12}$ changes phase from α to β and from β to γ, respectively [137]. The results clearly indicated that the addition of fillers led to a reduction in the crystallinity and an improvement in the porosity of the pristine GPEs, subsequently enhancing their conductivity. Among the CGPEs tested, the one incorporating γ-$Na_4Sc_2P_2SiO_{12}$ fillers exhibited the highest conductivity at 2.783 × 10^{-3} S·cm^{-1}, a sodium ion transference number (t_{Na+}) of 0.57, an impressive electrochemical window of 5.27 V, and an exceptionally low activation energy of just 0.0320 eV. This specific CGPE performed exceptionally well in Na/CGPE/$Na_3Sc_2P_3O_{12}$ batteries, boasting an initial discharge specific capacity of 92.3 mAh·g^{-1} and retaining 98.18% of its capacity after 100 cycles. The CGPE-containing β-$Na_{3.5}Sc_2P_{2.5}Si_{0.5}O_{12}$ fillers exhibited a very good conductivity as high as 2.072 × 10^{-3} S·cm^{-1}, a t_{Na+} of 0.47, an electrochemical window of 5.17 V, and a modest activation energy of 0.0328 eV. It also demonstrated a promising electrochemical performance, with an initial discharge specific capacity of 93.8 mAh·g^{-1} and a capacity retention rate of 97.87% after 100 cycles.

In contrast, the CGPE-incorporating α-$Na_3Sc_2P_3O_{12}$ filler performed less favorably when compared to the β- and γ-crystal forms. It exhibited a narrower electrochemical window of 5.07 V, a lower t_{Na+} of 0.35, a conductivity of 1.92 × 10^{-3} S·cm^{-1}, and a slightly higher activation energy of 0.0370 eV. Its capacity retention rate after 100 cycles was 97.20%, and it displayed an initial discharge specific capacity of 93 mAh·g^{-1}. This study underscores the significance of modifying the crystal structure (α-, β-, and γ-) of $Na_3Sc_2P_3O_{12}$ for improving the performance of GPEs.

Kim et al. [138] introduced a method to engineer the inner porous nanostructure of a PVDF-HFP polymer in GPEs for SIBs supported by glass fibers (GFs) using non-solvent-induced phase separation (NIPS). In terms of both the pore nanostructure and vertical position of the PVDF-HFP film, various types of porous GPEs inside the GF matrix exhibited different SIB performances. The improved GPEs in the GFs allowed for a higher ionic conductivity and exhibited superior cell properties with an excellent stability. The authors found various advantages depending on the morphology and placement of the porous PVDF-HFP film in the GF. During the phase inversion of PVDF-HFP, DI water and methanol served as pore inducers and positioners, respectively, in a binary non-solvent system. This resulted in a GPE with a uniform ion transport pathway for more uniform utilization of the electrode materials and a minimized interfacial resistance for effective ionic migration from electrolyte to electrode and vice versa. The electrochemical performance of the SIBs, in terms of their long cycling and high current density, was enhanced due to the synergic effects of two non-solvents, resolving the issue of parasitic capacity decay. This drawback

has been a persistent one for SIBs in previous studies due to the use of hollow GF structures. The proposed approach enables the production of cost-effective GPEs for SIB.

Kim et al. [139] used a cathode made of poly(2,2,6,6-tetramethylpiperidine-4-yl-1-oxyl vinyl ether) (PTVE) along with a microporous GPE based on an electrospun polyimide membrane to demonstrate an advanced organic radical battery (ORB). PTVE was used to functionalize carbon nanotubes (CNTs) via a dissolution–diffusion procedure to increase the low electrical conductivity of these nanostructures (65 weight % PTVE and 35 weight % CNT). The PTVE-functionalized CNTs could be shaped into a dense electrode with acceptable porosity due to $\pi - \pi^*$ interactions between the two components. PTVE (3 wt%) was added as a binder in place of traditional non-conducting materials. The GPE was highly compatible with the desired microporosity.

An ORB based on the PTVE-CNT composite electrode, the above-mentioned GPE, and a hard carbon anode exhibited a good rate capability and stable cycling. The battery was endowed with 100% coulombic efficiency, zero self-discharge, and discharging capacities of 128.6 and 68.2 $mAh{\cdot}g^{-1}$ at 0.5 C and 10 C, respectively. Therefore, the resulting SIB is suitable for various high-power applications and is safe, light, and environmentally friendly.

Shin et al. [140] demonstrated that a cross-linked fibrous CGPE based on polyacrylonitrile (PAN) and mesoporous methacrylate-functionalized SiO_2 nanoparticles effectively encases a liquid electrolyte without experiencing any solvent leakage. This same CGPE exhibited advantageous interfacial characteristics and showed excellent cycling performance. A study by Aravindan et al. [141] revealed substantial enhancements in both the mechanical stability and ionic conductivity of a PVDF-HFP polymer membrane with the incorporation of 10% $AlO(OH)_n$. Nevertheless, it was observed that when the filler content surpassed a specific threshold, the nano-sized fillers exhibited a pronounced surface effect and a propensity to cluster together. Aggregated fillers can damage the ion conducting pathways, resulting in a drop in the ionic conductivity of the PE [142].

With the addition of 1-(4-cyanophenyl)-guanidine, Zhao et al. [143] improved the ion conductive properties of a GPE and gave rise to an adjustable porous 3D network structure (a CGPE). PVDF-HFP provides a pathway for the transport of sodium ions within the system, and the imino nitrogen atom of 1-(4-cyanophenyl)guanidine is a ligand for sodium ions which facilitates the conduction of Na^+. The resulting CGPE (called PSGGSE) is characterized by a stable interface layer with the anode and an ionic conductivity of 0.232 $mS{\cdot}cm^{-1}$ at 70 °C. After 400 h of cycling of a symmetric Na/PSGGSE/Na cell at various current densities, no short circuit was observed, indicating that PSGGSE can successfully stop the formation of Na dendrites. Additionally, the Na/PSGGSE/$NiMoO_4$ battery exhibited superior cycling stability at a 100 $mAh{\cdot}g^{-1}$ current density and continued to have a high capacity of 150 $mAh{\cdot}g^{-1}$ after 200 cycles. The authors were able to produce a tunable porous structure and improved interface stability with the addition of SnO_2 fillers. The PSGGSE exhibited a high t_{Na^+} (0.58), high conductivity (0.232 $mS{\cdot}cm^{-1}$), and high cycling performance in a symmetric cell configuration (Na/PSGGSE/Na). Additionally, the PSGGSE/anode interface was studied using SEM imaging, confirming that the electrode material was prevented from pulverizing due to volume expansion associated with the charging and discharging processes.

A porous composite polymer membrane was prepared from a GPE based on a blend of PEO, PMMA, and PVDF-HFP and nano-sized oxide fillers (Al_2O_3, TiO_2, and SiO_2) by Shi et al. [144]. The CGPE containing SiO_2 fillers exhibited several advantageous characteristics. It possessed increased amorphous regions and a porous structure that could effectively accommodate more liquid electrolyte without leakage. Moreover, it showed higher cationic transport numbers for both Li^+ and Na^+, resulting in an improved ionic conductivity. The CGPE, prepared using a solvent casting technique, also offered a substantial electrochemical stability window, strong interfacial stability, and enhanced thermal resilience. The ion transport numbers of the CGPEs were determined through a combination of chronoamperometry and electrochemical impedance spectroscopy (EIS)

analysis in Li/GPE/Li or Na/GPE/Na cells [145]. The pores and amorphous structure of the CGPEs increased as a result of the oxide fillers and the segmental motion of the polymer chain. The unique structure of these CGPEs was closely associated with their remarkable interfacial and electrochemical stability, impressive ionic conductivity, and a substantial capacity to hold liquid electrolytes. The presence of nano-sized particles played a crucial role in preserving the mechanical strength of the solid electrolyte interphase (SEI) coating and stabilizing the interface between the CGPE and alkali metal anode. These findings suggest that CGPEs incorporating nanoscale SiO_2 fillers represent a promising choice for rechargeable Li or Na metal batteries, offering improved safety and an extended cycle life.

A study by Zhu et al. [146] reports the successful production of a porous composite membrane in which a nonwoven P(VDF-HFP) membrane supported by polypropylene serves as the reinforcing material while P(VDF-HFP) acts as the polymer host. Notably, the tensile strength of this membrane closely resembles that of the Celgard 2730 separator in both wet and dry conditions. At ambient temperature, it was measured that the ionic conductivity (0.82 $mS{\cdot}cm^{-1}$) was four times greater than that of the commercial separator (0.16 $mS{\cdot}cm^{-1}$) saturated with the same electrolyte. Additionally, it was shown that the Na^+ ion transference number was quite high, and the liquid electrolyte was retained even at 110 °C. The aforementioned CGPE was used to study the electrochemical reversibility of a $Na_4Mn_9O_8$ cathode, as confirmed using cyclic voltammetry. The porous CGPE has excellent application potential for high-energy-density SIBs. As shown in earlier publications, phase inversion was used to prepare the porous PVDF-HFP membrane [147]. The transference number of sodium ions (t_{Na^+}) within the CGPE was measured using a combination of AC and DC approaches [148]. In conclusion, the porous composite GPE exhibits excellent application potential for large-capacity SIBs.

High energy densities in SMBs are theoretically possible, but severe sodium dendrite growth and side reactions make them impractical for use, especially at high temperatures. Lei et al. [149] designed an inorganic ionic conductor/GPE composite in which evenly cross-linked beta alumina nanowires are compactly coated by a GPE based on P(VDF-HFP) due to their reciprocal strong molecular interactions. Together with the gel polymer layer, these beta alumina nanowires generate dense and uniform solid–liquid hybrid sodium ion transportation channels that facilitate uniform sodium deposition and the development of a flat, stable, solid electrolyte interface on the sodium metal anode. SiO_2 additives were added to the above-mentioned GPEs to further enhance their characteristics [150], commercial glass fiber (GF) membranes [151], and polydopamine (PDA) [152].

In their study, Gao et al. [152] demonstrated that SIBs can be significantly improved through the integration of an economical composite gel polymer/glass fiber electrolyte. This CGPE consists of PVDF-HFP reinforced with a glass fiber paper which underwent modification with a polydopamine coating to fine-tune the mechanical and surface properties of the perfluorinated polymer. The resulting composite polymer matrix displayed exceptional mechanical strength and thermal stability, remaining stable even at temperatures as high as 200 °C.

After being saturated with a liquid electrolyte, the CGPEs exhibited a wide electrochemical window and strong ionic conductivity. When tested using a sodium ion battery with $Na_2MnFe(CN)_6$ as the cathode material, significant enhancements were observed in the rate capability, cycle performance, and coulombic efficiency. These findings suggest that this CPE could be highly beneficial in large-scale battery systems where safety and cost-efficiency are primary concerns, particularly when employed with a dual function as a separator. The precipitation process previously described was used to prepare the cathode material for $Na_2MnFe(CN)_6$ [153,154]. The glass fiber paper was used to impart the composite GPEs with a high thermal stability and good mechanical strength. The polydopamine coating was useful for expanding the electrochemical window, which enabled the use of the CPEs with different electrode designs and enhanced the ionic conductivity. Sodium ion half-cells with $Na_2MnFe(CN)_6$ as the cathode performed much better electrochemically when the CGPEs were used. The authors anticipated that the integrated strategy used for

CGPEs can easily be applied to other polymer and battery systems, ultimately enhancing the performance of other energy storage technologies.

In Na-S and Na-nickel chloride batteries that operate at 300–350 °C, polycrystalline Na beta alumina (Na-β-Al_2O_3) with a strong ionic conductivity and good thermal characteristics is employed as the solid electrolyte material. A straightforward procedure was used to prepare the NVP cathode material in accordance with earlier research [155]. Cross-linked β/β''-Al_2O_3 nanowire membranes were produced using an electrospinning technique and then heated through an annealing process. Thanks to the effective immobilization of the electrolyte facilitated by ANs-GPE and the establishment of a stable and flat solid electrolyte interphase (SEI) on the sodium (Na) metal anode, undesired side reactions between the Na metal anode and the liquid electrolyte, as well as the formation of Na dendrites, were successfully mitigated. Remarkably, even after 1000 cycles at 1 C and 60 °C, the Na/ANs-GPE/NVP cell exhibited impressive capacity retention, maintaining a rate of 78.8%. This study introduced the concept of solid–liquid hybrid sodium ion transport channels within hybrid electrolytes composed of ceramic electrolytes and GPEs. This innovative approach could also be adapted for use in batteries containing lithium (Li), potassium (K), or other metal ions.

A CGPE was formulated by Luo et al. [156] primarily using graphene oxide (GO) and PVDF-HFP. Notably, the compressive Young's modulus of the sample, specifically the one containing 2 wt% GO within the PVDF-HFP matrix, referred to as the 2-GPH composite GPE, exhibited a remarkable tenfold increase, reaching 2.5 GPa. This significant boost in modulus plays a crucial role in preventing the formation of sodium dendrites. Consequently, under high current density conditions (5 $mA{\cdot}cm^{-2}$), the 2-GPH CGPE enabled uniform sodium deposition and achieved exceptionally long-lasting reversible sodium plating and stripping, extending beyond 400 h. Full SMBs were assembled from the metal sodium anode, NVP [157] cathode, and a number of electrolytes, such as 2-GPH GPE, PH GPE, and a LE. Additionally, the GO content enhanced the movement of sodium ions, as shown using a molecular dynamics simulation, leading to a high ionic conductivity of 2.3×10^{-3} $S{\cdot}cm^{-1}$. An impressive initial capacity of 107 $mAh{\cdot}g^{-1}$ was obtained when the composite GPE was combined with a $Na_3V_2(PO_4)_3$ cathode in a complete sodium metal battery. After 1100 cycles, the capacity retention rate was high at 93.5%, and the coulombic efficiency was high at 99.8%.

Mishra et al. [158] studied the impact of Al_2O_3 nanoparticle dispersion on the ionic conductivity of a non-aqueous PVDF-HFP/PMMA blend-based nanocomposite GPE (NGPE) containing a sodium trifluoromethanesulfonate liquid electrolyte. The ionic conductivity of the pristine GPE was measured to be 7.5×10^{-4} $S{\cdot}cm^{-1}$. Different Al_2O_3 concentrations in the PVDF-HFP/PMMA were introduced, and the NGPE considerably altered the ionic conductivity of the system. The composition, including 6 weight percent Al_2O_3 nanoparticles, caused the ionic conductivity of the electrolyte to increase to a maximum of 1.5×10^{-3} $S{\cdot}cm^{-1}$. A VTF behavior was observed for the optimum composition in the temperature range of 50 to 95 °C. Al_2O_3 nanoparticles were uniformly distributed throughout the porous structure of the NGPE, and the amorphicity of the polymer matrix increased, as shown by SEM and XRD studies. The faster conduction of the dissociated ions of the liquid electrolyte trapped in the PVDF-HFP/PMMA matrix, as well as the amorphous gel phase, both contributed to the increased conductivity. The composition with the highest conductivity had a Na^+ transport number of 0.30 and a significant electrochemical stability window of 3.6 V. These characteristics imply the viable application of the improved NGPE for SBs and supercapacitors. Using a Na-Hg/P-C cell (P-C is phosphorus-activated carbon) and the highest conducting NGPE composition, a prototype sodium battery was assembled. The battery exhibited a capacity reduction with cycling, an open circuit voltage of 2.5 V, and a first discharge capacity of 400 $mAh{\cdot}g^{-1}$. Measurements made utilizing EIS, LSV, CV, and chronoamperometry were used in the electrochemical investigations of the NGPEs. Due to significant thickening in the passivation layer, which raised the cell's internal resistance, a serious capacity fading was observed during cycling.

In general terms, the major focus on the synthesis of Na GPEs represents a tacit admission that Na SPEs have not met expectations. The awareness of the fact that organic liquid electrolytes such as EC and PC maintain their mainstream practical significance has led researchers towards the development of Na GPEs similar to Li GPEs. The trapping of EC, PC, or similar organic liquids in three-dimensional structures is a proven, clever strategy for preventing liquid leakage and preserving liquid-like conductivity. Thus far, the polymer host of choice seems to be PVDF-HFP. This perfluorinated copolymer seems to provide the most reliable confinement for liquid electrolytes. An aspect that we find interesting is that PVDF is a well-known piezoelectric material. Therefore, we wonder if the presence of PVDF is also associated with voltage-dependent electrostatic assistance to the conductivity process. The employment of fluorine-containing anions is expected to cause their preferential interaction with the perfluorinated polymer host. The use of PMMA in the assembly of electrolytes seems to be related mostly to the ease with which it can be polymerized in a variety of conditions. The use of inorganic fillers in the context of GPEs has proceeded in parallel to the development of CPEs, as discussed in the next section.

2.3. Composite Polymer Electrolytes (CPEs)

SPEs consist of a polymer matrix containing sodium salt and no liquid solvent. Unfortunately, SPEs suffer from a low ionic conductivity. The advancement of this field relies on the following approaches: (1) reducing the percentage of liquid plasticizers [159] and (2) adding inorganic fillers [32]. As explained above, we consider plasticized polymer electrolytes (PPEs) to be separate from CPEs, which include inorganic fillers. The physical properties of the components used in these types of CPEs are displayed in Figure 7. The use of these strategies in some cases comes at the price of sacrificing part of the mechanical, thermal, and chemical stability of SPEs. The addition of inorganic ceramic fillers seems to be the most promising route, as it usually increases ionic conductivity.

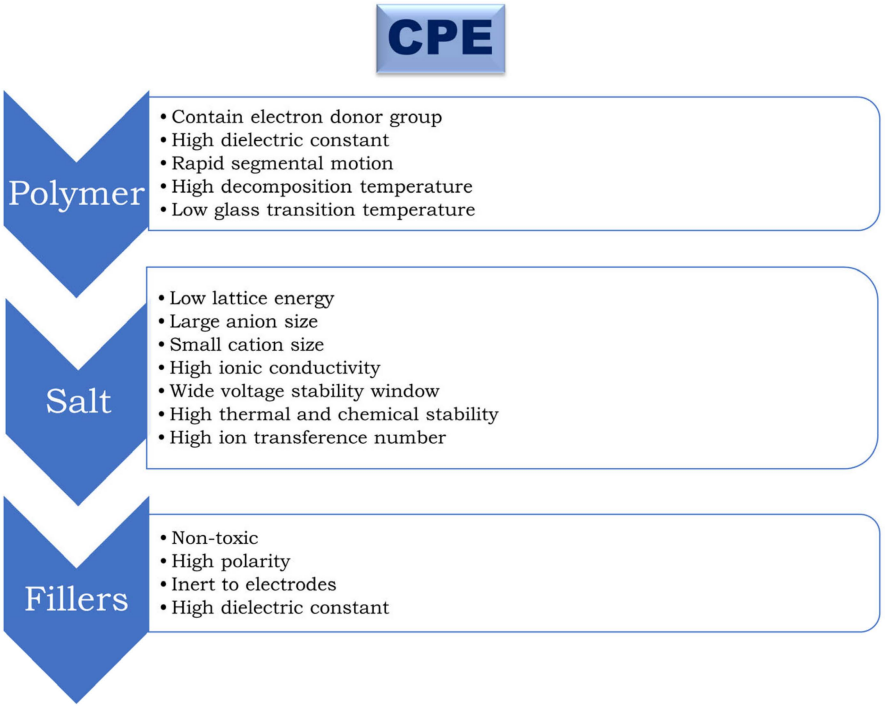

Figure 7. Composite polymers electrolytes.

An ideal CPE should have a high ionic conductivity (up to the order of 10^{-3} S·cm^{-1}) in a wide temperature range to enable SIBs with a high cycle and rate performance (Figure 8). The following list of targeted requirements are desirable characteristics in CPEs. (1) In order to prevent sluggish reactions with the electrodes during the processes of sodium insertion

and extraction, it is crucial for CPEs to possess a wide electrochemical stability range of up to 5 V. (2) To prevent deformation while operating at high temperatures, CPEs should have a strong dimensional stability and superior thermal stability of up to at least 150 °C. The deformation of PEs in SIBs generally results in significant risks including short circuits and thermal runaway due to the poor thermal stability of conventional PEs. (3) In order to achieve optimal power performance and mitigate issues related to ionic concentration polarization, CPEs should exhibit a high sodium ion (t_{Na+}) transference number, ideally close to 1. Additionally, these CPEs need to possess substantial mechanical strength to effectively deter the penetration of sodium dendrites. (4) Mechanical robustness is a crucial attribute for CPEs, especially when considering their applications in wearable and flexible energy storage devices. (5) CPEs in SIBs ought to be cost-effective for a wide range of energy storage applications. (6) To ensure the safe and long-term supply of SIBs, CPEs should exhibit a low toxicity and should be comprised of materials that are abundant on Earth. It is important to bridge the gap between the actual performance of a practical electrolyte and the structural, chemical, and functional qualities of an ideal CPE [160].

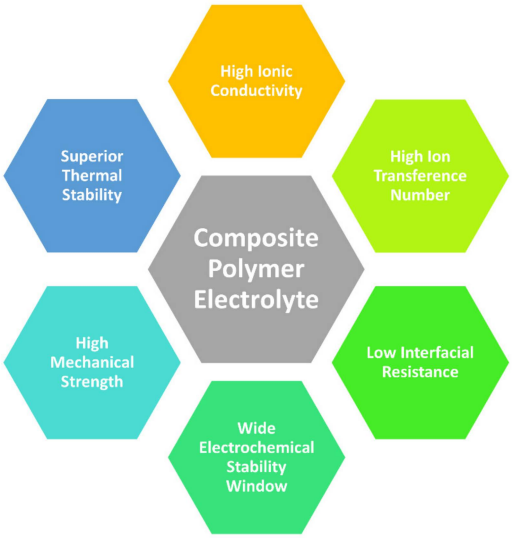

Figure 8. Characteristic properties of composite polymers electrolytes.

It was discovered that GPEs filled with various inorganic oxides, including SiO_2, Al_2O_3, TiO_2, ZrO_2, $BaTiO_3$, etc. [161–163] showed enhanced mechanical strength, higher ionic conductivity, and improved electrochemical stability of the Li/electrolyte interface compared to those without filling. These systems were labelled CGPE in the previous section. Similarly, the direct dispersion of active or inert inorganic oxide fillers within PEs without plasticizers leads to the formation of CPEs. Given that active fillers directly participate in the ion conduction process, their incorporation generally leads to increased conductivity and a greater mobile ion transference number compared to inert fillers.

In 2015, Ni'mah et al. [164] reported PEs based on PEO using a transition metal oxide filler for SIBs. Initially the PEO/TiO_2 nanocomposite was prepared followed by the synthesis of the cathodic material $Na_{2/3}Co_{2/3}Mn_{1/3}O_2$ using the carbonate co-precipitation method. The maximal ionic conductivity of a SPE with an equilibrium ratio of EO:Na = 20 is 1.35 × 10^{-4} S·cm^{-1}, which increases to 2.62 × 10^{-4} S·cm^{-1} when TiO_2 (3.4 nm, 5 wt%) is added at a temperature of 60 °C.

A study by Verma et al. [165] investigated the dispersion of TiO_2 nanofillers in Na-conducting nanocomposite polymer electrolyte membranes. The base material for the membranes was PVDF-HFP. Initially, TiO_2 was immersed in a liquid electrolyte comprising $NaPF_6$ and EC. The membranes containing TiO_2 were then prepared using the phase inversion technique. It was discovered that the membranes were quite porous, with a maximum porosity of ~72% and a liquid electrolyte uptake of ~270%. It was determined

using complex impedance spectroscopy that the highest ionic conductivity at room temperature was ~1.3×10^{-3} S·cm^{-1}. It was found that the ionic conductivity, measured as a function of temperature, exhibited VTF behavior. DC polarization, complex impedance, and cyclic voltammetry were used to probe the electrochemical properties of the CPEs. It was determined that the membranes contained a Na^+ transport number of approximately 0.31. The electrochemical stability window of the membranes was 3.5 V. The pore density reached its maximum at 0.50 weight percent TiO_2, and the pore size grew with TiO_2 content.

Zhang et al. [166] described the preparation of a CPE for SIBs that are entirely solid-state. The sol-gel process was used to synthesize $Na_3V_2(PO_4)_3$ (NVP) using carbon nanotubes as the cathode material (NVP@CNTs). A novel electrolyte comprised of a PMMA/PEG hybrid polymer with 5% nano-Al_2O_3 was produced and first used in SIBs. The CPE performed quite well, and the following three characteristics stood out: (i) at 70 °C, a comparatively high ionic conductivity of 1.46×10^{-4} S·cm^{-1} was attained; (ii) there was minimal anodic breakdown, even at 4.5 V vs. Na^+/Na; and (iii) the mechanical flexibility of the CPEs assured intimate contact with the electrodes. The all-solid-state SIBs showed a high reversible capacity of 85 mAh·g^{-1} at 0.5 C and a 94.1% capacity retention after 350 cycles.

In 2018, Jinisha et al. [51] reported a PEO:$NaNO_3$ PE with an Al_2O_3 filler, which exhibited its highest conductivity of 1.86×10^{-4} S·cm^{-1} at room temperature. The first solid CPEs based on PEO and NaTFSI with an active ceramic filler (NASICON) were described by Zhang et al. [167]. The incorporation of NASICON fillers significantly improved both the thermal and electrochemical stability of the electrolytic complexes. A CPE with NASICON filler content of 50% by weight showed the highest conductivity of 2.8 mS·cm^{-1} (at 80 °C). Furthermore, solid-state batteries constructed using a sodium (Na) anode, CPE as the electrolyte, and $Na_3V_2(PO_4)_3$ as the cathode exhibited an excellent rate performance and impressive cycling stability. The NASICON electrolyte was synthesized using the sol-gel process, and $Na_3V_2(PO_4)_3$ was produced via a solid-state reaction [168]. NASICON ($Na_{1+x}Zr_2Si_xP_{3-x}O_{12}$, $0 \leq x \leq 3$) ceramic electrolytes have been previously researched for their excellent ionic conductivity, thermal stability, and broad electrochemical window [169].

Zhao et al. [170] studied PVDF-HFP, 1-butyl-3-methylimidazolium tetrafluoroborate ($BMIMBF_4$), and NaSCN that were electrospun as composite nanofibrous electrolyte membranes (CFEM). The interconnected multifibrous layers and ultrathin porous architectures of the electrospun CFEM and CFEM-NaSCN fibers were investigated using SEM. The fibers had an average diameter of 50–200 nm and showed substantial electrolyte solution absorption (370–880%). The decrease in crystallinity of the PEs was accompanied by a rise in their ionic conductivity. The composite material CFEM, incorporating 15% BMIMBF4, demonstrated a peak ionic conductivity of 5.6×10^{-5} S·cm^{-1} at room temperature. The CPEs exhibited Arrhenius behavior. In comparison to electrospun pure PVDF-HFP without $BMIMBF_4$ or $BMIMBF_4$-NaSCN, the CFEM-NaSCN electrolyte exhibited an increased electrochemical window, surpassing 4.5 V. It is expected that the CFEM electrolyte and the CFEM-NaSCN electrolyte are suitable for high-performance rechargeable batteries and super capacitors due to their outstanding performance characteristics. The $BMIMBF_4$, an RTIL, was synthesized using a previously described method [171]. The preparation of CFEM and CFEM-NaSCN involved electrospinning, and the porous materials were immersed in an ionic electrolyte solution to produce the CPEs [172].

Song et al. [173] presented a CPE made by sandwiching poly(ethylene oxide) (PEO)-based PE between nanoporous ceramic layers. A superior ionic conductivity of 1.6×10^{-4} S·cm^{-1} at ambient temperature, stable Na plating and stripping, as well as a wide electrochemical stability window of 4.2 V versus Na/Na^+ were made possible using this laminated arrangement.

In 2017, Lee et al. [174] reported on the thermal and electrical conductivity properties of a PE composed of PEO, $NaClO_4$, and barium titanate ($BaTiO_3$) as a filler. They noted that the addition of $BaTiO_3$ further enhanced the conductivity, reaching a maximum value of 1.0×10^{-5} S·cm^{-1} at room temperature.

Moreno et al. [175] prepared membranes of NaTFSI complexed with PEO with various EO:Na molar ratios. Above 70 °C, all the membranes exhibited excellent ionic conductivities of approximately 10^{-3} S·cm^{-1}. Due to the anion's plasticizing properties, the samples with higher concentrations of NaTFSI exhibited a sticky gum-like behavior. A compromise in the conductivity, thermal, and mechanical properties could be seen in the PEO_{20}:NaTFSI sample. The mechanical properties of the PEO_{20}:NaTFSI membranes were further improved by the addition of nanometric SiO_2. Additionally, the PEO_{20}:NaTFSI membranes with 5 weight percent SiO_2 demonstrated a similar anodic electrochemical stability and ionic conductivity to the ceramic-free PEO_{20}:NaTFSI sample. When compared to a ceramic-free membrane, the addition of the ceramic filler significantly increased the interfacial resistance in a Na/PE/Na symmetrical cell that was monitored for 30 days. The anion and cation diffusion coefficients determined using NMR indicated that the presence of a filler may have had a favorable impact on the cation transference number (t_{Na^+}), which was consistent with the electrochemical measurements. The neutralization reaction between HTFSI and Na_2CO_3 in aqueous solution was used to synthesize the sodium salt [176]. PEO_n:NaTFSI PEs were prepared via a hot pressing (solvent-free) method [177]. These membranes exhibited conductivity and stability values that made them very promising materials for use as electrolytes in cutting-edge SIBs with innovative designs, particularly for grid applications requiring rapid production. Additional work is being carried out to confirm this expectation, particularly with the PEO_n:NaFSI system.

Kunteppa et al. [178] synthesized other PEO-based composites by stirring PEO and polyaniline in anhydrous acetonitrile for 5 to 6 h to create homogenous solutions or gels with various weight percentages. FTIR and SEM were used to characterize the composites. The formation of PEO:PANI:$NaClO_4$ composites was confirmed based on the main peaks in the FTIR spectra. Based on the SEM measurements, the morphology of the CPEs with different weight percentages of $NaClO_4$ significantly changed, going from ellipsoidal to square features. The hopping of polarons from one localized state to another, which is supported by Mott theory, contributed to the ionic DC conductivity that was observed. These composites can be excellent candidates for solid-state electrolytes, as seen in investigations of the DC conductivity and SEM.

Chen et al. [179] proposed a novel solid electrolyte named B-CPE (boron-modified CPE) which was designed for SIBs. B-CPE was prepared through in situ polymerization within a mechanically supportive matrix. This electrolyte exhibited an exceptional ionic conductivity at 40 °C, measuring 2.57×10^{-4} S·cm^{-1}, along with a high sodium-ion (Na^+) transference number of 0.66. It also demonstrated excellent compatibility with the sodium (Na) metal anode. This improvement was attributed to the formation of a continuous ion-conducting polymer phase, facilitated by a one-step in situ solidification process that fostered a suitable contact between the electrode and electrolyte interface.

Solid-state SIBs based on B-CPE displayed an outstanding electrochemical performance by leveraging the synergy of a high-performance electrolyte and an optimized cell design. The best-performing SIB exhibited an initial discharge capacity of 113.8 mAh·g^{-1} and retained 80.1% of its capacity after 320 cycles at 40 °C at 0.2 C and 80.4% after 700 cycles at 3 C. Notably, the addition of boron moieties significantly improved the battery's rate capability. This research paves the way for the development of high-performance rechargeable solid-state batteries. The cathode material, $NaNi_{1/3}Fe_{1/3}Mn_{1/3}O_2$ (NFM), was prepared using a traditional solution casting technique, consisting of NFM active material/PVDF binder/Super-P in a ratio of 80/10/10 w/w/w. The NFM active material synthesis followed prior methods [180].

A novel CPE known as PVC-CPE based on poly(vinylene carbonate) was developed by Chen et al. [181] for the assembly of high-performance solid-state SBs that operate at room temperature. The PVC-CPE was solidified in situ and exhibited several favorable characteristics including enhanced stability at the electrode/electrolyte interface, a high sodium ion (Na^+) transference number (t_{Na+} = 0.60), and superior ionic conductivity (0.12 mS·cm^{-1} at 25 °C). Significantly, a composite cathode, $NaNi_{1/3}Fe_{1/3}Mn_{1/3}O_2$ (*c*-

NFM), was designed to minimize interfacial resistance and facilitate efficient ion transport across the electrode/electrolyte interfaces. This achievement was realized by forming the PE in situ within the electrode. In comparison to a reference sodium/PVC-CPE/*c*-NFM battery produced using a conventional ex situ approach, the solid-state sodium/PVC-CPE/*c*-NFM battery demonstrated markedly improved cell performance at room temperature. The device exhibited a high initial specific capacity of 104.2 $mAh \cdot g^{-1}$ at 0.2 C, retained 86.8% of its capacity over 250 cycles, and maintained a capacity of 80.2 $mAh \cdot g^{-1}$ at 1 C. PVC-CPE emerges as a highly promising electrolyte for solid-state SIBs.

A study was conducted by Ahad et al. [182] on the structural, thermal, and electrical characteristics of solid CPEs comprised of poly(vinyl alcohol) complexed with sodium salicylate. These CPEs were fabricated through a solution casting method, utilizing various weight-to-percentage ratios. Analysis using XRD revealed that the concentration of sodium salicylate resulted in an expansion of the amorphous regions within the polymer. It was observed that the breakdown of these CPEs decreased as the amount of sodium salicylate increased.

The electrical properties, including the conductivity and dielectric characteristics, were investigated. This analysis was carried out over a temperature range spanning from 303 K to 343 K and in the frequency range 20 Hz to 1 MHz. The results indicated that as both the temperature and sodium salicylate concentration increased, the conductivity of the CPEs also increased. Additionally, the dielectric constant increased with rising temperatures, while the dielectric loss decreased with higher sodium salicylate contents. The PVA-50 wt% sodium salicylate sample showed the best conductivity, lowest activation energy, highest amorphous nature, and highest thermal stability, making it perfect for application in electrochemical devices.

Yu et al. [183] investigated a CPE that integrates the flexibility characteristics of a PE with the high ionic conductivity found in ceramic electrolytes. A simple slurry-casting technique was used to create a composite electrolyte containing PEO, $NaClO_4$ salt, and a ceramic Na ion conductor ($Na_3Zr_2Si_2PO_{12}$) scattered in it. The resulting CPE showed increased dendrite suppression, improved electrode/electrolyte interface, and an elastic consistency. All-solid-state batteries with a sodium metal anode, PEO/$NaClO_4$/$Na_3Zr_2Si_2PO_{12}$ as an electrolyte, and a $Na_2MnFe(CN)_6$ cathode exhibited a stable long-term cycling performance. The polymer/ceramic composite was prepared using a straightforward slurry-casting technique to disperse a nanoparticle electrolyte material, $Na_3Zr_2Si_2PO_{12}$, into the PEO and sodium perchlorate. At a high temperature of 60 °C, the PEO/$NaClO_4$/$Na_3Zr_2Si_2PO_{12}$ CPE exhibited a Na ion conductivity of 5.6×10^{-4} $S \cdot cm^{-1}$. Long-term electrochemical stability and compatibility with the Na metal anode and the $Na_2MnFe(CN)_6$ cathode were demonstrated by the PEO/$NaClO_4$/$Na_3Zr_2Si_2PO_{12}$ electrolyte membranes. Due to their capacity to suppress the sodium dendrites during sodium plating, the $Na_3Zr_2Si_2PO_{12}$ nanoparticles considerably increased the stability of the Na/PEO-$NaClO_4$-$Na_3Zr_2Si_2PO_{12}$/Na symmetric cells. The Na/PEO-$NaClO_4$-$Na_3Zr_2Si_2PO_{12}$/$Na_2MnFe(CN)_6$ cells, which were entirely solid-state, presented a respectable rate capability and long-term cycle stability. The findings of this study show that the polymer/ceramic composite is a promising approach for the assembly of all-solid-state SBs.

Wang et al. [184] employed thin layers of ferroelectrics as a distinctive approach to customize the interfaces between electrodes and an all-solid-state CPE. An ionic conductivity of 7.9×10^{-5} $S \cdot cm^{-1}$ was recorded at ambient temperature. The incorporation of ferroelectric engineering also improved ion transport across the electrolyte–ferroelectric cathode/anode interfaces, effectively suppressing the formation of the SEI between the CPEs and the Na metal electrodes. Notably, after 165 cycles at room temperature, an exceptionally high discharge capacity of 160.3 $mAh \cdot g^{-1}$ with 97.4% retention was attained in the ferroelectric-engineered all-solid-state Na metal cell. Furthermore, despite the cell having been aged for two months, a remarkable stability was shown based on the high discharge capacity retention of 86.0% after 180 complete charge/discharge cycles. This research offers fresh perspectives on how to improve the stability and long-cyclability of

solid-state rechargeable batteries. NZSP ceramic frameworks with pores [185] and a KNN precursor solution [186] were prepared as described earlier. The interfacial ion transport at the electrolyte–ferroelectric–cathode/anode interfaces was improved, and the SEI growth was successfully inhibited.

In 2021, Dimri et al. [187] reported the study of a PE based on PEO and sodium triflate ($NaCF_3SO_3$) in conjunction with zinc ferrite ($ZnFe_2O_4$) nanoparticles. $ZnFe_2O_4$ was prepared via the citrate combustion method using the precursors zinc nitrate, ferric nitrate, and citric acid. The PE was prepared by adding ferrite nanoparticles to PEO and $NaCF_3SO_3$ in the presence of PC as plasticizer. This CPE was characterized as a film, and the ferrite nanoparticles were found to increase the amorphicity of the system. The conductivity of the electrolyte was 6×10^{-5} S·cm^{-1} at room temperature. In the same year, Chauhan et al. [188] reported the enhancement of ion transport in PE based on PEO and $NaClO_4$ using sodium aluminate ($NaAlO_2$) as fillers. The addition of 5 wt% of $NaAlO_2$ filler increased the electrolyte conductivity from 1.6×10^{-5} S·cm^{-1} at 25 °C to 7.4×10^{-5} S·cm^{-1} at 30 °C. Similarly, in the same year, Yao et al. [189] reported the effects of the addition of 10 wt% of β-alumina as fillers to PEO/$NaClO_4$, which was found to increase the conductivity from 2.5×10^{-4} to 3.95×10^{-4} S·cm^{-1} at 60 °C. Again, in 2021, Mallaiah et al. [190] reported the impact of PVDF blending with PEO/$NaNO_3$ and found that PVDF addition increased the conductivity to 9.334×10^{-5} S·cm^{-1} at room temperature for PEO:PVDF:$NaNO_3$ in a ratio of 80:20:5.

A solution casting process was used by Pradhan et al. [191] to produce a plasticized CPE (PCPE) based on PEO, NaI, and Na_2SiO_3 as the ceramic filler and PEG as the plasticizer. Investigations were performed to understand how plasticization affects the electrical and microscopic structure of the material. Utilizing XRD and SEM studies, it was determined how the addition of plasticizer alters the surface morphology and increases the concentration of amorphous materials. DSC showed that the presence of plasticizers reduces the internal viscosity of the polymers and increases their flexibility. With an increase in the plasticizer content, it was discovered that the grain boundary resistance decreased. At room temperature, adding the plasticizer caused the conductivity value to increase by a factor of three. The conductivity as a function of the reciprocal temperature demonstrates a thermally activated process of the Arrhenius type above and below the melting temperature T_m of PEO.

Na CPEs represent a compromise between the properties of SPEs and those of inorganic fillers. Both PVDF and PEO have been used in this context. It is interesting that PEO becomes immediately relevant, though not exclusively, the moment that the use of liquid solvent additives is not allowed. PVDF and PEO can interact with nanosized oxides of different kinds through their respective polar moieties. It appears that the nanoparticles are quite effective in disrupting the long-range crystallinity of the polymer host. At the same time, they mediate local interactions of regions of the polymer host, which provide partially charged nanodomains that assist the motion of Na^+ cations. One issue of concern in Na CPEs is whether a true integration of the components occurs rather than a more or less stable formation of multiphasic materials with different ion conduction pathways.

3. Conclusions and Future Perspectives

Since 2010, the field of SIBs has shown widespread interest, and the related number of publications has been growing tremendously. The discovery of new electrolytes and the improvement of existing ones play a crucial role in the advancement of this area of research and development. The specific choice of electrolyte has a significant impact not only on the energy density and cycle life of batteries, but also their manufacturing processes, cost, and safety. Given the thermodynamic differences between sodium and lithium, the development of electrolytes for SIBs cannot solely rely on the experience gained from LIBs. PE-based SBs provide unique opportunities not only to reduce raw material costs but also to enhance the inherent safety of the batteries. Over the past 35 years, there has been a significant increase in the variety of Na ion-conducting polymer

matrices, sodium salts, and plasticizers or fillers, leading to notable advancements in the physicochemical and electrochemical properties. PEs offer the potential to merge the advantages of solid electrolytes, such as rigidity and durability, with the high ionic conductivity of soft-matter electrolytes. Furthermore, PEs are associated with additional benefits such as flame resistance, absence of leakage or volatility, flexibility, thermal stability, and electrochemical stability, all of which have the potential to enable robust battery technologies. The need to establish PE-based SIBs is quite pressing due to safety concerns and the limitation of lithium resources. Herein, we present an extensive examination of Na PEs designed for use in both primary and secondary SBs. The emphasis is placed on solid, gel, and composite polymer electrolytes, which are characterized by specific compromises of advantages and disadvantages (see Figure 9). The comparison of the conductivity versus temperature of the SPE, GPE, and CPE systems reviewed in this paper are presented in Figure 10. Similar information with additional details is given in Tables 1–3.

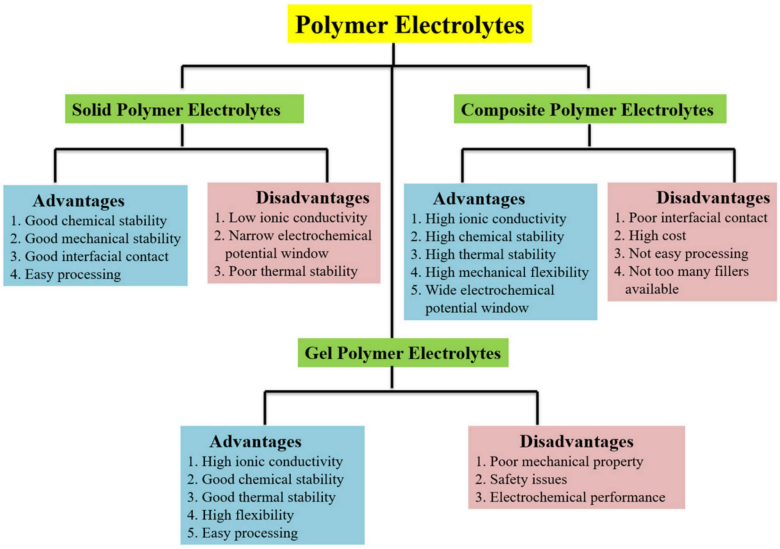

Figure 9. Advantages and disadvantages of SPEs, GPEs, and CPEs.

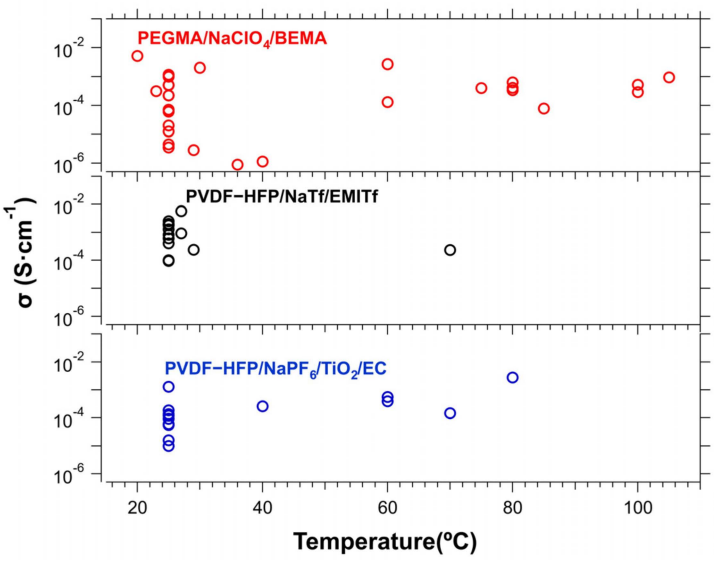

Figure 10. Comparison of conductivity of the PEs reviewed in this article. The formulas of the top-performing PEs are indicated. Lists of these materials are given in Tables 1–3.

Table 1. Comparison of SPEs in terms of conductivity.

Year	SPE	Temp	Conductivity	Ref
1995	PEO + $NaPF_4$	25 °C	5×10^{-6} S·cm^{-1}	[53]
1999	PEO + $NaNO_3$	29 °C	2.83×10^{-6} S·cm^{-1}	[54]
2001	PEO + $NaClO_3$ + PEG	105 °C	9.47×10^{-4} S·cm^{-1}	[55]
2005	PEO + $NaNO_3$	25 °C	3.5×10^{-6} S·cm^{-1}	[52]
2006	PEO + $NaClO_3$	~30 °C	~10^{-7} S·cm^{-1}	[56]
2006	PEO + $NaFeF_4$	25 °C	1.37×10^{-7} S·cm^{-1}	[57]
2006	PVC + $NaClO_4$	-	-	[71]
2006	PVA + NaBr	-	1.12×10^{-6} S·cm^{-1}	[74]
2007	PEO + $NaLaF_4$	25 °C	3.9×10^{-7} S cm^{-1}	[58]
2007	$(PEO)_6$:$NaPO_3$ + PEG400	36 °C	8.9×10^{-7} S cm^{-1}	
2007	PVA + NaI	-	1.02×10^{-5} S·cm^{-1}	[73]
2012	PEO + NaF	-	4.73×10^{-7} S cm^{-1}	[61]
2013	Potato starch + NaSCN	-	1.12×10^{-4} S·cm^{-1}	[44]
2014	HPMC + NaI	40 °C	1.126×10^{-6} S·cm^{-1}	[81]
2015	MC + NaI	60 °C	2.7×10^{-5} S·cm^{-1}	[82]
2015	BEMA/PEGMA + $NaClO_4$	20 °C	5.1×10^{-3} S·cm^{-1}	[13]
2015	MPII + RS + NaI	-	1.20×10^{-3} S·cm^{-1}	[77]
2016	PEO + sodium methylsulfate salt + BMIM-MS	75 °C	4×10^{-4} S·cm^{-1}	[85]
2017	PEO + NaFNFSI	80 °C	3.36×10^{-4} S·cm^{-1}	[62]
2017	PEO + NaI	25 °C	7.1×10^{-5} S·cm^{-1}	[63]
2017	PVC + NaI	25 °C	2.9×10^{-8} S·cm^{-1}	[72]
2017	Tri(ethylene glycol) divinyl ether + $LiBF_4$	Ambient temperature	1.2×10^{-3} S·cm^{-1}	[86]
2017	Poly(bis(4-carbonyl benzene sulfonyl)imide-co-2,5-diamino benzesulfonic acid) + NaPA	80 °C	4.1×10^{-4} S·cm^{-1}	[87]
2017	CS + NaCl	-	1.72×10^{-5} S·cm^{-1}	[78]
2018	PVA + $NaNO_3$ + PVP	25 °C	1.25×10^{-5} S·cm^{-1}	[75]
2018	Oligo(methyl methacrylate)-block-oligo(ethylene glycol) methyl ether methacrylate + H-β-CD + NaTFSI	60 °C	1.3×10^{-4} S·cm^{-1}	[88]
2019	PEO + $NaPF_6$	25 °C	2×10^{-5} S·cm^{-1}	[64]
2019	PEO + $NaNO_3$ + PVP	100 °C	2.90×10^{-4} S·cm^{-1}	[65]
2019	PVDF + $NaPF_6$	Ambient temperature	1.08×10^{-3} S·cm^{-1}	[89]
2019	(P(MVE-*alt*-MA)) + TEP/VC + $NaClO_4$	25 °C	2.2×10^{-4} S·cm^{-1}	[90]
2020	PEO + PEI + $NaPF_6$	100 °C	5.2×10^{-4} S·cm^{-1}	[66]
2020	PEO + $NaPF_6$ + succinonitrile	80 °C	6.3×10^{-4} S·cm^{-1}	[67]
2020	PEO + Na(FSI-ethyl cellulose)	80 °C	~10^{-4} S·cm^{-1}	[68]
2020	CMC-Na + PVP	-	1.81×10^{-4} S·cm^{-1}	[83]
2020	CMC + NaBr	25 °C	5.15×10^{-4} S·cm^{-1}	[84]
2020	MC + NaI	-	3.01×10^{-3} S·cm^{-1}	[46]
2021	PVA + NaI + Glycerol	25 °C	1.17×10^{-3} S·cm^{-1}	[76]
2021	CS-$NaHSO_3$	25 °C	2.22×10^{-4} S·cm^{-1}	[79]
2021	Chitosan/Dextran + $NaCF_3SO_3$	25 °C	6.10×10^{-5} S·cm^{-1}	[80]
2021	TMPT crosslinked with NaBFMB	30 °C	2×10^{-3} S cm^{-1}	[91]
2022	PEO + NaFSI + $Pyr_{14}FSI$	25 °C	1×10^{-3} S·cm^{-1}	[69]
2022	PEO + NaCl	25 °C	4.5×10^{-6} S·cm^{-1}	[70]
2022	PVDF + NaTFSI + NaDFOB	23 °C	3.1×10^{-4} S·cm^{-1}	[92]
2023	PEO + $NaClO_4$ + $NaCF_3SO_3$	90 °C	10^{-3} S·cm^{-1}	[93]
2023	PEO + PNaMTFSI	85 °C	7.74×10^{-5} S·cm^{-1}	[94]

Table 2. Comparison of GPEs in terms of conductivity.

Year	GPE	Temp	Conductivity	Ref
1981, 2021	PVDF-HFP/PMMA- γ-$Na_4Sc_2P_2SiO_{12}$ β-$Na_{3.5}Sc_2P_{2.5}Si_{0.5}O_{12}$ α-$Na_3Sc_2P_3O_{12}$	- - -	2.783×10^{-3} S·cm^{-1} 2.072×10^{-3} S·cm^{-1} 1.92×10^{-3} S·cm^{-1}	[136,137]
2004	PVDF + PSVE-Na + PC + VA	Ambient temperature	Above 10^{-4} S.cm^{-1}	[118]
2010	PVDF-HFP + NaTf + EMITf	~27 °C	5.74×10^{-3} S·cm^{-1}	[121]
2016	PAN + NaI + EC + DMF	29 °C	2.35×10^{-4} S·cm^{-1}	[134]
2017	PPC + NaI + EC:PC	25 °C	2.01×10^{-3} S·cm^{-1}	[133]
2017	P(VDF-HFP) + $NaClO_4$ + PP	Ambient temperature	8.2×10^{-4} S·cm^{-1}	[146]
2018	P(VDF-co-HFP) + $NaClO_4$ + EC + DEC	-	1.13×10^{-3} S·cm^{-1}	[127]
2019	PVDF-HFP + $NaCF_3SO_3$ + PMMA	25 °C	~6.1×10^{-4} S·cm^{-1}	[124]
2019	PSP + $NaClO_4$ + PSTB + PVCA	25 °C	1×10^{-4} S·cm^{-1}	[110]
2019	PVDF-HFP + $NaClO_4$ + PC + FEC	25 °C	1.91×10^{-3} S·cm^{-1}	[112]
2019	PVDF-HFP/PMMA + $NaCF_3SO_3$ + EC + PC		7.5×10^{-4} S·cm^{-1}	[157]
2020	PVDF-HFP/PMMA + $Na_2Zn_2TeO_6$ + ED + DMC	25 °C	2.52×10^{-3} S·cm^{-1}	[109]
2020	PPEGMA + NaTFSI + TEP	27 °C	9.1×10^{-4} S·cm^{-1}	[114]
2020	poly(acrylonitrile-co-methyl acrylate) + $NaClO_4$ + PC	25 °C	1.8×10^{-3} S·cm^{-1}	[117]
2020	PVDF-HFP + NaPTAB + EC + PC	25 °C	9.4×10^{-5} S·cm^{-1}	[128]
2020	CPN + $NaPF_6$ + PC	25 °C	8.2×10^{-4} S·cm^{-1}	[132]
2020	2-GPH + $NaClO_4$ + EC + PC	-	2.3×10^{-3} S·cm^{-1}	[156]
2021	PVDF-HFP/PMMA + $Ti_3C_2T_x$ MXene + $NaClO_4$ + EC + DMC	-	3.28×10^{-3} S·cm^{-1}	[111]
2021	PVDF-HFP + $NaCF_3SO_3$ + $BMImCF_3SO_3$	25 °C	4.0×10^{-4} S·cm^{-1}	[113]
2021	PVDF-HFP + NaTFSI + EMIMTFSI	-	1.9×10^{-3} S·cm^{-1}	[123]
2021	PVDF-HFP + $NaAlO_2$ + EC + PC	-	6.8×10^{-4} mS·cm^{-1}	[125]
2021	PVDF-co-HFP + $NaPF_6$ + EC + PC	25 °C	1.28×10^{-3} S·cm^{-1}	[126]
2021	PCL-TA + NaFSI + TMP	-	6.3×10^{-3} S·cm^{-1}	[131]
2022	PVDF-HFP + $NaClO_4$ + G3	-	2.54×10^{-3} S·cm^{-1}	[119]
2022	TMP + $NaPF_6$ + EC + PC	-	~1.40×10^{-3} S·cm^{-1}	[123]
2022	PVDF-HFP-PSGGSE- SnO_2 + $NaClO_4$ + EC + DMC	70 °C	2.32×10^{-4} S·cm^{-1}	[143]

Table 3. Comparison of CPEs in terms of conductivity.

Year	CPE	Temp	Conductivity	Ref
2013	P(VDF-HFP) + NaSCN + $BMIMBF_4$ Not mentioned	25 °C	5.6×10^{-5} S·cm^{-1}	[170]
2014	PEO + NaTFSI + SiO_2	>75 °C	~10^{-3} S·cm^{-1}	[175]
2015	PEO + $NaClO_4$ + TiO_2	25 °C	1.35×10^{-4} S·cm^{-1}	[164]
2017	PEO + $NaClO_4$ + $BaTiO_3$	25 °C	1.0×10^{-5} S·cm^{-1}	[174]
2017	PEO + NaTFSI + NASICON	80 °C	2.8 mS·cm^{-1}	[167]
2018	PMMA/PEG + $NaClO_4$ + Al_2O_3	70 °C	1.46×10^{-4} S·cm^{-1}	[166]
2018	PEO + $NaNO_3$ + Al_2O_3	25 °C	1.86×10^{-4} S·cm^{-1}	[51]
2019	PEO + $NaClO_4$ + $Na_3Zr_2Si_2PO_{12}$	60 °C	5.6×10^{-4} S·cm^{-1}	[183]
2020	PVDF-HFP + $NaPF_6$ + TiO_2 + EC	25 °C	1.3×10^{-3} S·cm^{-1}	[165]
2021	PEGMA + NaTF + B-HEMA + TEGDME	40 °C	2.57×10^{-4} S·cm^{-1}	[179]
2021	PEO + $NaCF_3SO_3$ + $ZnFe_2O_4$	25 °C	6×10^{-5} S·cm^{-1}	[187]
2021	PEO + $NaClO_4$ + $NaAlO_2$	25 °C	1.6×10^{-5} S·cm^{-1}	[188]
2021	PEO + $NaClO_4$ + β-Al_2O_3	60 °C	3.95×10^{-4} S·cm^{-1}	[189]
2022	PEO + NaTFSI + KNN-$Na_3Zr_2Si_2PO_{12}$	Ambient temperature	7.9×10^{-5} S·cm^{-1}	[184]

SPEs are based on the solvent-aided or solvent-free dissolution of salts into polymer hosts. Na ion-conducting SPEs have been proposed since the beginning of this area of research. The preferred polymers have been PEO, PEG, PEI, PMMA, PVP, PVC, PVA, RS, MC, HPMC, CMC, PVDF, PVDF-HFP, and P(MVE-*alt*-MA). Salts have included sodium halides, NaF, NaCl, NaBr, NaI, $NaNO_3$, NaSCN, $NaPF_6$, $NaBF_4$, $NaClO_3$, $NaClO_4$, $NaPO_3$, NaTf, NaFSI, NaTFSI, NaFNFSI, $NaFeF_4$, $NaLaF_4$, NaBFMB, and NaDFOB. These systems do not present very high conductivities in comparison to organic liquid electrolytes, but they do exhibit a wide electrochemical window, higher chemical and thermal stabilities, and reduced flammability. Additionally, they are conducive to a simplified battery design. Modifications of SPEs with ILs yielding PILE systems and photocrosslinking of the anions with the polymer host have been explored. The improvement of the ionic conductivity of SPEs has been relying on the control of salts and polymer matrices. However, understanding the characteristics of electrode/electrolyte interfaces, especially the SPE/sodium electrode interface that critically influences overall cell performance, cannot be straightforwardly predicted solely based on the molecular structure and interactions of the electrolyte components. Comprehensive investigations involving both experimental and computational approaches are essential to unravel these aspects.

GPEs provide higher ionic conductivities, approaching those of organic liquid electrolytes. However, challenges persist related to the leakage and volatilization of the incorporated liquid solvent, which can negatively impact the durability of these materials. Polymer networks have been synthesized using PVB, PAN, PMMA, PVC, PVDF, PVDF-HFP, P(AN-*co*-MA), PPEGMA, vinyl acetate, perfluoro(5-methyl-3,6-dioxo-8-fluoride sulfonyl-1-octene), polycaprolactone triacrylate, cross-linked polyethers, and PTVE. The organic liquids used have included EC, PC, PPC, PGC, DEC, FEC, DMF, 1-(4-cyanophenyl)-guanidine, and dicinnamylidene hexanediamine. ILs such as EMImTf, BMImTFSI, and solvate ionic liquids such as [Na-(glyme)]ClO_4 have been considered as additives. The salts that have been employed have included NaI, $NaClO_4$, $NaPF_6$, NaTf, NaTFSI, and NaPTAB. The addition of Na-containing or non-Na-containing inorganic fillers such as SiO_2, TiO_2, SnO_2, Al_2O_3, $AlO(OH)_n$, Na-β-Al_2O_3, NASICON (i.e., $Na_{3+x}Sc_2P_{3-x}Si_xO_{12}$ with x = 0, 0.5, and 1.0), $Na_2Zn_2TeO_6$, $NaAlO_2$, and $Ti_3C_2T_x$ MXenes have resulted in viable CGPE materials. The use of a small percentage of GO proved to be beneficial to the preparation of a CGPE. Stabilization using a glass fiber was also an interesting strategy that was employed. The use of the flame retardants TMP and TEP imparted improved thermal stability. Epichlorohydrin with titanium/silicon alkoxy compounds was used to synthesize hybrid inorganic organic CGPEs early on in this field. Despite significant advancements in gel polymer SIBs, practical applications still face challenges. The long-term cycle life of assembled half-cells is a crucial criterion for evaluating commercial battery performance. Currently, only a limited number of GPE-based SIBs exhibit a lifespan exceeding 1000 cycles, particularly with hard carbon and other anode materials. Additionally, achieving synergy between electrolytes and electrode materials is crucial for commercialization. This involves optimizing storage capacity and working voltage, matching suitable GPEs, and enhancing the stability and consistent application of the entire battery system. The integration of GPEs with environmentally friendly electrodes holds promise for advanced applications in various fields.

CPEs consist of PEs stabilized by inorganic fillers. The polymers that have been investigated include PEO, PEG, PVDF-HFP, PMMA, and PVA. The fillers were chosen among SiO_2, TiO_2, Al_2O_3, $NaAlO_2$, Na_2SiO_3, NASICON (i.e., $Na_{1+x}Zr_2Si_xP_{3-x}O_{12}$, $0 \leq x \leq 3$), $BaTiO_3$, $Na_3Zr_2Si_2PO_{12}$, and $ZnFe_2O_4$. Boron-based CPEs were also studied. The salts included NaI, $NaNO_3$, $NaPF_6$, NaFSI, NaTf, NaTFSI, $NaClO_4$, and NaSCN. Engineering approaches have focused on the use of glass fibers for the mechanical stabilization of CPEs, the introduction of ferroelectrics to modulate the electrolyte–electrode interface, and the use of the IL $BMIMBF_4$ for electrospinning. Despite achieving desired Na ion conductivity, electrochemical properties, mechanical strength, and a well-established electrode–electrolyte contact in composite electrolytes, challenges persist in transitioning from the lab to industry.

Scientists grapple with the practical application of CPEs in SIBs, asking for new paradigms and efforts to bridge the experimental–commercial gap. Key challenges include addressing low ionic conductivity to meet the performance of highly conductive liquid electrolytes. Exploration of novel polymer materials and fillers with high ionic conductivities is essential. Tuning host polymers for CPEs using rational engineering techniques to enhance ionic conductivity and employing functionalization recipes like copolymerization, cross-linking, and grafting are crucial. Cost minimization is vital for large-scale SIB manufacturing, urging accelerated use of low-cost materials, bio-inspired polymers, and sustainable precursors. Additionally, designing innovative electrolyte systems is essential for constructing flexible, transparent, and electrochromic SIBs.

The best performance of Na batteries was measured using GPEs and CPEs as electrolytes. The best capacity was based on NGPEs in a Na-Hg/P-C cell. The open circuit voltage was 2.5 V, and the first discharge capacity was 400 mAh·g^{-1}. The best capacity based on CPEs was measured for a sodium/PVC-CPE/*c*-NFM battery at 104.2 mAh·g^{-1}. Therefore, GPE-based batteries appear to be the most significant in terms of practical applications.

It is expected that future research will extend to the study of tensile strength, shear strength, and elongation in the entire operational temperature range and not just under ambient conditions. More research is needed on PE to avoid or reduce dendrite formation. A clearer understanding is required concerning the underlying dynamics of dendrite formation. Studies focused on improving the interfacial layer between PEs and electrodes and methods for enhancing interfacial contact are highly desirable. Furthermore, additional exploration of hybrid inorganic–organic PEs may reveal new pathways for higher performance Na ion-conducting systems.

Taken together, increasing the ionic conductivity in Na ion-conducting SPEs, GPEs, and CPEs seems to have become an asymptotic process with an obvious ceiling. Optimization of these materials in isolation is not sufficient. The synthesis and characterization of PEs need to be understood and carried out in relation to the other specific components of fully assembled SIB systems. Applying high-throughput screening analysis techniques to extensive sets of electrolyte formulations, coupled with a combination of theoretical, electrochemical, and spectroscopic methods, can significantly accelerate the exploration and optimization process. There is a pressing need for a systematic approach to design electrolytes for future SIBs.

Author Contributions: Conceptualization, M.V.; writing—original draft preparation, S.K., R.R. and M.V.; writing—review and editing, S.K., R.R. and M.V.; funding acquisition, M.V. All authors have read and agreed to the published version of the manuscript.

Funding: This research was funded by Natrion Incorporated and the ASRC CUNY Sensor Center for Advanced Technology (Grant numbers 72957-00 01 and 55440-01 04, respectively).

Acknowledgments: The authors dedicate this manuscript to Ashok Prasad of the University of Delhi, advisor of S.K., who has recently passed away. The authors would like to thank CEO Alex Kosyakov (Natrion) and Director of Business Development Tavis Ezell (CUNY Sensor CAT). The authors thank Virinder Parmar for his advisory role.

Conflicts of Interest: The authors declare no conflicts of interest.

Abbreviations

AC	Activated charcoal
AC	Alternating current
AFM	Atomic force microscopy
AGPE	Amorphous gel polymer electrolyte
Al_2O_3	Aluminum oxide
ASIB	Aqueous sodium ion battery

$BaTiO_3$	Barium titanate
BET	Brunauer–Emmett–Teller
$BMIMBF_4$	1-*butyl*-3-methylimidazolium tetrafluoroborate
BMIM-MS	1-*butyl*-3-methylimidazolium methylsulfate
CFEM	Composite nanofibrous electrolyte membranes
CMC	Carboxy methylcellulose
CNT	Carbon nanotubes
CPE	Composite polymer electrolyte
CPN	Crosslinked polyether network
CS	Cornstarch
DC	Direct current
DEC	Diethyl carbonate
DI	Deionized
DMA	Dynamic mechanical analysis
DMF	Dimethyl formamide
DMSO	Dimethylsulfoxide
DSC	Differential scanning calorimetry
DSSC	Dye-sensitized solar cells
EC	Ethylene carbonate
EDLC	Electric double-layer capacitor
EDS	Energy dispersive spectroscopy
EES	Electrochemical energy storage
EIS	Electrochemical impedance spectroscopy
ESW	Electrochemical stability window
$Fe(NO_3)_3$	Ferric nitrate
FEC	Fluoroethylenecarbonate
FESEM	Field emission scanning electron microscopy
FTIR	Fourier transform–infrared spectroscopy
FTO	Fluoride/tin oxide
GO	Graphene oxide
GPC	Gel permeation chromatography
GPE	Gel polymer electrolyte
HOMO	Highest occupied molecular orbital
HPMC	Hydroxypropyl methylcellulose
HSCR	Hydrothermal soft chemical reaction
H-β-CD	Hyperbranched β-cyclodextrin
IL	Ionic liquid
IR	Infrared
kΩ	Kiloohms
$La(NO_3)_3$	Lathanum nitrate
LE	Liquid electrolyte
LIB	Lithium ion battery
LSV	Linear sweep voltammetry
LUMO	Lowest unoccupied molecular orbital
MC	Methylcellulose
MHz	Megahertz
MPII	1-methyl-3-propylimidazolium iodide
MW	Molecular weight
$NaAlO_2$	Sodium aluminate
NaBFMB	Bis(fluoroallyl)malonato borate salt
NaBr	Sodium bromide
$NaCF_3SO_3$	Sodium triflate
$NaCF_3SO_3$	Sodium trifluoromethanesulfonate
$NaClO_3$	Sodium chlorate

NaDFOB	Sodium-difluoro(oxalato)borate
NaF	Sodium fluoride
$NaHSO_3$	Sodium hydrogen sulfite
NaI	Sodium iodide
$NaNO_3$	Sodium nitrate
NaPA	Poly(*bis*(4-carbonyl benzene sulfonyl)imide-co-2,5-diamino benzesulfonic acid)
$NaPF_2$	Sodium difluorophosphate
$NaPF_6$	Sodium hexafluorophosphate
NaPTAB	Sodium-poly(tartaric acid)borate
NaSCN	Sodium thiocyanate
NaTFSI	Sodium trifluoromethaneslfonimide
NGPE	Nanocomposite gel polymer electrolytes
NIPS	Non-solvent-induced phase separation
NMR	Nuclear magnetic resonance
ORB	Organic radical battery
P(MVE-alt-MA)	Poly(methyl vinyl ether-*alt*-maleic anhydride)
PAN	Poly(acrylonitrile)
PANI	Polyaniline
PC	Propylene carbonate
PCPE	Platicizer composite polymer electrolyte
PDA	Polydopamine-plastcized polyne
PE	Polymer electrolyte
PEG	Poly(ethylene glycol)
PEGMA	Poly(ethylene glycol) methyl ether methacrylate
PEM	Proton exchange membrane
PEO	Poly(ethylene) oxide
PFSA	Perfluorosulfonic acid
PILEs	Polymer ionic liquid electrolytes
PMMA	Poly(methyl methacrylate)
PPEGMA	Poly(poly(ethylineglycol)methacrylate)
PTVE	2,2,6,6-tetramethylpiperidine-4-yl-1-oxyl vinyl ether
PVA	Poly(vinyl alcohol)
PVB	Poly(vinyl butyral)
PVC	Poly(vinyl chloride)
PVDF	Poly(vinylidene fluoride)
PVDF-HFP	Poly(vinylidene fluoride hexafluoro propylene)
PVP	Poly(vinyl pyrolidone)
RT	Room temperature
RTIL	Room-temperature ionic liquid
SAED	Selected area electron diffraction
SIB	Sodium ion battery
SEI	Solid electrolyte interphase
SEM	Scanning electron microscopy
SGPE	Separator-cum gel polymer electrolyte
SHE	Standard hydrogen electrode
SIC	Single ion-conducting
SIL	Solvate ionic liquid
SMB	Sodium metal battery
SPE	Solid polymer electrolyte
TEP	Triethyl phosphate
TGA	Thermogravimetric analyzer
TG-DTA	Thermogravimetric differential thermal analysis
TiO_2	Titanium dioxide

TMP	Trimethyl phosphate
TMPT	Tri-thiol (trimethylolpropane tris(3-mercapto propionate)
VC	Vinylene carbonate
VTF	Vogel–Tammann–Fulcher
Wh	Watt-hour
XPS	X-ray photoelectron spectroscopy
XRD	X-ray diffraction
$ZnFe_2O_4$	Zinc ferrite

References

1. Yang, Z.; Zhang, J.; Kintner-Meyer, M.C.W.; Lu, X.; Choi, D.; Lemmon, J.P.; Liu, J. Electrochemical Energy Storage for Green Grid. *Chem. Rev.* **2011**, *111*, 3577–3613. [CrossRef] [PubMed]
2. Armand, M.; Tarascon, J.M. Building better batteries. *Nature* **2008**, *451*, 652–657. [CrossRef] [PubMed]
3. Goodenough, J.B.; Park, K.-S. The Li-Ion Rechargeable Battery: A Perspective. *J. Am. Chem. Soc.* **2013**, *135*, 1167–1176. [CrossRef] [PubMed]
4. Tarascon, J.M.; Armand, M. Issues and challenges facing rechargeable lithium batteries. *Nature* **2001**, *414*, 359–367. [CrossRef] [PubMed]
5. Goodenough, J.B.; Kim, Y. Challenges for Rechargeable Li Batteries. *Chem. Mater.* **2010**, *22*, 587–603. [CrossRef]
6. Yang, R.; Zhang, F.; Lei, X.; Zheng, Y.; Zhao, G.; Tang, Y.; Lee, C.-S. Pseudocapacitive Ti-Doped Niobium Pentoxide Nanoflake Structure Design for a Fast Kinetics Anode toward a High-Performance Mg-Ion-Based Dual-Ion Battery. *ACS Appl. Mater. Interfaces* **2020**, *12*, 47539–47547. [CrossRef]
7. Lei, X.; Zheng, Y.; Zhang, F.; Wang, Y.; Tang, Y. Highly stable magnesium-ion-based dual-ion batteries based on insoluble small-molecule organic anode material. *Energy Storage Mater.* **2020**, *30*, 34–41. [CrossRef]
8. Vignarooban, K.; Kushagra, R.; Elango, A.; Badami, P.; Mellander, B.E.; Xu, X.; Tucker, T.G.; Nam, C.; Kannan, A.M. Current trends and future challenges of electrolytes for sodium-ion batteries. *Int. J. Hydrogen Energy* **2016**, *41*, 2829–2846. [CrossRef]
9. Deng, X.; Zou, K.; Cai, P.; Wang, B.; Hou, H.; Zou, G.; Ji, X. Advanced Battery-Type Anode Materials for High-Performance Sodium-Ion Capacitors. *Small Methods* **2020**, *4*, 2000401. [CrossRef]
10. Hwang, J.-Y.; Myung, S.-T.; Sun, Y.-K. Sodium-ion batteries: Present and future. *Chem. Soc. Rev.* **2017**, *46*, 3529–3614. [CrossRef]
11. Peters, J.F.; Peña Cruz, A.; Weil, M. Exploring the Economic Potential of Sodium-Ion Batteries. *Batteries* **2019**, *5*, 10. [CrossRef]
12. Xu, G.-L.; Amine, R.; Abouimrane, A.; Che, H.; Dahbi, M.; Ma, Z.-F.; Saadoune, I.; Alami, J.; Mattis, W.L.; Pan, F. Challenges in Developing Electrodes, Electrolytes, and Diagnostics Tools to Understand and Advance Sodium-Ion Batteries. *Adv. Energy Mater.* **2018**, *8*, 1702403. [CrossRef]
13. Bella, F.; Colò, F.; Nair, J.R.; Gerbaldi, C. Photopolymer Electrolytes for Sustainable, Upscalable, Safe, and Ambient-Temperature Sodium-Ion Secondary Batteries. *ChemSusChem* **2015**, *8*, 3668–3676. [CrossRef] [PubMed]
14. Nayak, P.K.; Yang, L.; Brehm, W.; Adelhelm, P. From Lithium-Ion to Sodium-Ion Batteries: Advantages, Challenges, and Surprises. *Angew. Chem. Int. Ed.* **2018**, *57*, 102–120. [CrossRef] [PubMed]
15. Yang, J.; Zhang, H.; Zhou, Q.; Qu, H.; Dong, T.; Zhang, M.; Tang, B.; Zhang, J.; Cui, G. Safety-Enhanced Polymer Electrolytes for Sodium Batteries: Recent Progress and Perspectives. *ACS Appl. Mater. Interfaces* **2019**, *11*, 17109–17127. [CrossRef] [PubMed]
16. Jin, Y.; Sun, X.; Yu, Y.; Ding, C.; Chen, C.; Guan, Y. Research Progress in Sodium-Ion Battery Materials for Energy Storage. *Prog. Chem.* **2014**, *26*, 582–591.
17. Chayambuka, K.; Mulder, G.; Danilov, D.L.; Notten, P.H.L. Sodium-Ion Battery Materials and Electrochemical Properties Reviewed. *Adv. Energy Mater.* **2018**, *8*, 1800079. [CrossRef]
18. Delmas, C. Sodium and Sodium-Ion Batteries: 50 Years of Research. *Adv. Energy Mater.* **2018**, *8*, 1703137. [CrossRef]
19. Zhang, Z.; Zhang, Q.; Ren, C.; Luo, F.; Ma, Q.; Hu, Y.-S.; Zhou, Z.; Li, H.; Huang, X.; Chen, L. A ceramic/polymer composite solid electrolyte for sodium batteries. *J. Mater. Chem. A* **2016**, *4*, 15823–15828. [CrossRef]
20. Goodenough, J.B.; Hong, H.Y.P.; Kafalas, J.A. Fast Na+-ion transport in skeleton structures. *Mater. Res. Bull.* **1976**, *11*, 203–220. [CrossRef]
21. Qiao, L.; Judez, X.; Rojo, T.; Armand, M.; Zhang, H. Review—Polymer Electrolytes for Sodium Batteries. *J. Electrochem. Soc.* **2020**, *167*, 070534. [CrossRef]
22. Li, Z.-Y.; Li, Z.; Fu, J.-L.; Guo, X. Sodium-ion conducting polymer electrolytes. *Rare Met.* **2023**, *42*, 1–16. [CrossRef]
23. Jacobson, A.J.; Chianelli, R.R.; Rich, S.M.; Whittingham, M.S. Amorphous molybdenum trisulfide: A new lithium battery cathode. *Mater. Res. Bull.* **1979**, *14*, 1437–1448. [CrossRef]
24. Parant, J.-P.; Olazcuaga, R.; Devalette, M.; Fouassier, C.; Hagenmuller, P. Sur quelques nouvelles phases de formule $NaxMnO_2$ (x $\leq$ 1). *J. Solid State Chem.* **1971**, *3*, 1–11. [CrossRef]
25. Guo, G.; Hong, J.; Cong, C.; Zhou, X.; Zhang, K. Molybdenum disulfide synthesized by hydrothermal method as anode for lithium rechargeable batteries. *J. Mater. Sci.* **2005**, *40*, 2557–2559. [CrossRef]

26. Sarciaux, S.; Le Gal La Salle, A.; Verbaere, A.; Piffard, Y.; Guyomard, D. γ-MnO_2 for Li batteries: Part II. Some aspects of the lithium insertion process into γ-MnO_2 and electrochemically lithiated γ-Li_xMnO_2 compounds. *J. Power Sources* **1999**, *81–82*, 661–665. [CrossRef]
27. Mauger, A.; Julien, C.M.; Paolella, A.; Armand, M.; Zaghib, K. Building Better Batteries in the Solid State: A Review. *Materials* **2019**, *12*, 3892. [CrossRef]
28. Li, Q.; Chen, J.; Fan, L.; Kong, X.; Lu, Y. Progress in electrolytes for rechargeable Li-based batteries and beyond. *Green Energy Environ.* **2016**, *1*, 18–42. [CrossRef]
29. Eshetu, G.G.; Elia, G.A.; Armand, M.; Forsyth, M.; Komaba, S.; Rojo, T.; Passerini, S. Electrolytes and Interphases in Sodium-Based Rechargeable Batteries: Recent Advances and Perspectives. *Adv. Energy Mater.* **2020**, *10*, 2000093. [CrossRef]
30. Zhu, Z.; Chen, J. Review—Advanced Carbon-Supported Organic Electrode Materials for Lithium (Sodium)-Ion Batteries. *J. Electrochem. Soc.* **2015**, *162*, A2393. [CrossRef]
31. Fenton, D.E.; Parker, J.M.; Wright, P.V. Complexes of alkali metal ions with poly(ethylene oxide). *Polymer* **1973**, *14*, 589. [CrossRef]
32. Zhou, D.; Shanmukaraj, D.; Tkacheva, A.; Armand, M.; Wang, G. Polymer Electrolytes for Lithium-Based Batteries: Advances and Prospects. *Chem* **2019**, *5*, 2326–2352. [CrossRef]
33. Skaarup, S.; West, K.; Zachau-Christiansen, B. Mixed phase solid electrolytes. *Solid State Ionics* **1988**, *28–30*, 975–978. [CrossRef]
34. Hoang Huy, V.P.; So, S.; Hur, J. Inorganic Fillers in Composite Gel Polymer Electrolytes for High-Performance Lithium and Non-Lithium Polymer Batteries. *Nanomaterials* **2021**, *11*, 614. [CrossRef] [PubMed]
35. Huang, W.; Zhu, Z.; Wang, L.; Wang, S.; Li, H.; Tao, Z.; Shi, J.; Guan, L.; Chen, J. Quasi-Solid-State Rechargeable Lithium-Ion Batteries with a Calix[4]quinone Cathode and Gel Polymer Electrolyte. *Angew. Chem. Int. Ed.* **2013**, *52*, 9162–9166. [CrossRef] [PubMed]
36. Vasudevan, S.; Dwivedi, S.; Balaya, P. Overview and perspectives of solid electrolytes for sodium batteries. *Int. J. Appl. Ceram. Technol.* **2023**, *20*, 563–584. [CrossRef]
37. Ahmad, H.; Kubra, K.T.; Butt, A.; Nisar, U.; Iftikhar, F.J.; Ali, G. Recent progress, challenges, and perspectives in the development of solid-state electrolytes for sodium batteries. *J. Power Sources* **2023**, *581*, 233518. [CrossRef]
38. Zheng, J.; Li, W.; Liu, X.; Zhang, J.; Feng, X.; Chen, W. Progress in Gel Polymer Electrolytes for Sodium-Ion Batteries. *Energy Environ. Mater.* **2023**, *6*, e12422. [CrossRef]
39. Aruchamy, K.; Ramasundaram, S.; Divya, S.; Chandran, M.; Yun, K.; Oh, T.H. Gel Polymer Electrolytes: Advancing Solid-State Batteries for High-Performance Applications. *Gels* **2023**, *9*, 585. [CrossRef]
40. Maurya, D.K.; Dhanusuraman, R.; Guo, Z.; Angaiah, S. Composite polymer electrolytes: Progress, challenges, and future outlook for sodium-ion batteries. *Adv. Compos. Hybrid Mater.* **2022**, *5*, 2651–2674. [CrossRef]
41. Zhang, J.; Yue, L.; Hu, P.; Liu, Z.; Qin, B.; Zhang, B.; Wang, Q.; Ding, G.; Zhang, C.; Zhou, X. Taichi-inspired rigid-flexible coupling cellulose-supported solid polymer electrolyte for high-performance lithium batteries. *Sci. Rep.* **2014**, *4*, 6272. [CrossRef]
42. Tsuchida, E.; Ohno, H.; Tsunemi, K. Conduction of lithium ions in polyvinylidene fluoride and its derivatives—I. *Electrochim. Acta* **1983**, *28*, 591–595. [CrossRef]
43. Das, S.; Ghosh, A. Effect of plasticizers on ionic conductivity and dielectric relaxation of PEO-$LiClO_4$ polymer electrolyte. *Electrochim. Acta* **2015**, *171*, 59–65. [CrossRef]
44. Tiwari, T.; Srivastava, N.; Srivastava, P.C. Ion Dynamics Study of Potato Starch + Sodium Salts Electrolyte System. *Int. J. Electrochem.* **2013**, *2013*, 670914. [CrossRef]
45. Aragón, M.J.; Gutiérrez, J.; Klee, R.; Lavela, P.; Alcántara, R.; Tirado, J.L. On the effect of carbon content for achieving a high performing $Na_3V_2(PO_4)_3$/C nanocomposite as cathode for sodium-ion batteries. *J. Electroanal. Chem.* **2017**, *784*, 47–54. [CrossRef]
46. Aziz, S.B.; Brevik, I.; Hamsan, M.H.; Brza, M.A.; Nofal, M.M.; Abdullah, A.M.; Rostam, S.; Al-Zangana, S.; Muzakir, S.K.; Kadir, M.F.Z. Compatible Solid Polymer Electrolyte Based on Methyl Cellulose for Energy Storage Application: Structural, Electrical, and Electrochemical Properties. *Polymers* **2020**, *12*, 2257. [CrossRef] [PubMed]
47. Gao, H.; Zhou, W.; Park, K.; Goodenough, J.B. A Sodium-Ion Battery with a Low-Cost Cross-Linked Gel-Polymer Electrolyte. *Adv. Energy Mater.* **2016**, *6*, 1600467. [CrossRef]
48. Wang, Y.; Song, S.; Xu, C.; Hu, N.; Molenda, J.; Lu, L. Development of solid-state electrolytes for sodium-ion battery–A short review. *Nano Mater. Sci.* **2019**, *1*, 91–100. [CrossRef]
49. Moon, S.-H.; Kim, Y.H.; Cho, D.-C.; Shin, E.-C.; Lee, D.; Im, W.B.; Lee, J.-S. Sodium ion transport in polymorphic scandium NASICON analog $Na_3Sc_2(PO_4)_3$ with new dielectric spectroscopy approach for current-constriction effects. *Solid State Ion.* **2016**, *289*, 55–71. [CrossRef]
50. Faiz, H.; Zainuddin, S.K.; Kamarudin, K.; Kok Sheng, C.; Abdullah, M.A. Ion-conducting polymer electrolyte films based on poly (Sodium 4-styrenesulfonate) complexed with ammonium nitrate: Studies based on morphology, structural and electrical spectroscopy. *Malays. J. Anal. Sci.* **2018**, *22*, 238–248.
51. Jinisha, B.; Anilkumar, K.M.; Manoj, M.; Abhilash, A.; Pradeep, V.S.; Jayalekshmi, S. Poly (ethylene oxide) (PEO)-based, sodium ion-conducting, solid polymer electrolyte films, dispersed with Al_2O_3 filler, for applications in sodium ion cells. *Ionics* **2018**, *24*, 1675–1683. [CrossRef]
52. Anantha, P.S.; Hariharan, K. Physical and ionic transport studies on poly(ethylene oxide)–$NaNO_3$ polymer electrolyte system. *Solid State Ion.* **2005**, *176*, 155–162. [CrossRef]

53. Hashmi, S.A.; Chandra, S. Experimental investigations on a sodium-ion-conducting polymer electrolyte based on poly(ethylene oxide) complexed with $NaPF_6$. *Mater. Sci. Eng. B* **1995**, *34*, 18–26. [CrossRef]
54. Sreekanth, T.; Jaipal Reddy, M.; Ramalingaiah, S.; Subba Rao, U.V. Ion-conducting polymer electrolyte based on poly (ethylene oxide) complexed with $NaNO_3$ salt-application as an electrochemical cell. *J. Power Sources* **1999**, *79*, 105–110. [CrossRef]
55. Chandrasekaran, R.; Selladurai, S. Preparation and characterization of a new polymer electrolyte (PEO:$NaClO_3$) for battery application. *J. Solid State Electrochem.* **2001**, *5*, 355–361. [CrossRef]
56. Siva Kumar, J.; Subrahmanyam, A.R.; Jaipal Reddy, M.; Subba Rao, U.V. Preparation and study of properties of polymer electrolyte system (PEO+$NaClO_3$). *Mater. Lett.* **2006**, *60*, 3346–3349. [CrossRef]
57. Mohan, V.M.; Raja, V.; Sharma, A.K.; Narasimha Rao, V.V.R. Ion transport and battery discharge characteristics of polymer electrolyte based on PEO complexed with $NaFeF_4$ salt. *Ionics* **2006**, *12*, 219–226. [CrossRef]
58. Mohan, V.M.; Bhargav, P.B.; Raja, V.; Sharma, A.K.; Narasimha Rao, V.V.R. Optical and Electrical Properties of Pure and Doped PEO Polymer Electrolyte Films. *Soft Mater.* **2007**, *5*, 33–46. [CrossRef]
59. Bhide, A.; Hariharan, K. Ionic transport studies on $(PEO)_6$:$NaPO_3$ polymer electrolyte plasticized with PEG400. *Eur. Polym. J.* **2007**, *43*, 4253–4270. [CrossRef]
60. Bhide, A.; Hariharan, K. A new polymer electrolyte system $(PEO)_n$:$NaPO_3$. *J. Power Sources* **2006**, *159*, 1450–1457. [CrossRef]
61. Sasikala, U.T.; Kumar, P.N.; Rao, V.V.R.N.; Sharma, A.K. Structural, Electrical and Parametric studies of a PEO based Polymer Electrolyte for battery Applications. *Int. J. Eng. Sci. Adv. Technol.* **2012**, *2*, 722–730.
62. Ma, Q.; Liu, J.; Qi, X.; Rong, X.; Shao, Y.; Feng, W.; Nie, J.; Hu, Y.-S.; Li, H.; Huang, X. A new Na[(FSO_2)(n-$C_4F_9SO_2$)N]-based polymer electrolyte for solid-state sodium batteries. *J. Mater. Chem. A* **2017**, *5*, 7738–7743. [CrossRef]
63. Herath, H.M.A.; Seneviratne, V.A. Electrical and Thermal studies on Sodium based polymer electrolyte. *Procedia Eng.* **2017**, *215*, 124–129. [CrossRef]
64. Arya, A.; Sharma, A.L. Tailoring of the structural, morphological, electrochemical, and dielectric properties of solid polymer electrolyte. *Ionics* **2019**, *25*, 1617–1632. [CrossRef]
65. Pritam; Arya, A.; Sharma, A.L. Dielectric relaxations and transport properties parameter analysis of novel blended solid polymer electrolyte for sodium-ion rechargeable batteries. *J. Mater. Sci.* **2019**, *54*, 7131–7155. [CrossRef]
66. Pritam; Arya, A.; Sharma, A.L. Selection of best composition of Na^+ ion conducting PEO-PEI blend solid polymer electrolyte based on structural, electrical, and dielectric spectroscopic analysis. *Ionics* **2020**, *26*, 745–766. [CrossRef]
67. Zhang, Q.; Lu, Y.; Yu, H.; Yang, G.; Liu, Q.; Wang, Z.; Chen, L.; Hu, Y.-S. PEO-$NaPF_6$ Blended Polymer Electrolyte for Solid State Sodium Battery. *J. Electrochem. Soc.* **2020**, *167*, 070523. [CrossRef]
68. Youcef, H.B.; Orayech, B.; Del Amo, J.M.L.; Bonilla, F.; Shanmukaraj, D.; Armand, M. Functionalized cellulose as quasi single-ion conductors in polymer electrolyte for all-solid–state Li/Na and LiS batteries. *Solid State Ion.* **2020**, *345*, 115168. [CrossRef]
69. Kim, Y.; Künzel, M.; Steinle, D.; Dong, X.; Kim, G.-T.; Varzi, A.; Passerini, S. Anode-less seawater batteries with a Na-ion conducting solid-polymer electrolyte for power to metal and metal to power energy storage. *Energy Environ. Sci.* **2022**, *15*, 2610–2618. [CrossRef]
70. Chandra, A.; Chandra, A.; Dhundhel, R.S.; Bhatt, A. Sodium-ion-conducting solid polymer electrolyte: Temperature-dependent ionic parameters and solid-state polymer battery fabrication. *Indian J. Phys.* **2022**, *96*, 1069–1074. [CrossRef]
71. Subba Reddy, C.V.; Han, X.; Zhu, Q.-Y.; Mai, L.-Q.; Chen, W. Conductivity and discharge characteristics of (PVC+$NaClO_4$) polymer electrolyte systems. *Eur. Polym. J.* **2006**, *42*, 3114–3120. [CrossRef]
72. Muhammad, F.H.; Subban, R.H.Y.; Winie, T. Charge carrier density and mobility of poly(vinyl chloride)-based polymer electrolyte using impedance spectroscopy. *Mater. Today Proc.* **2017**, *4 Pt C*, 5130–5137. [CrossRef]
73. Bhargav, P.B.; Mohan, V.M.; Sharma, A.K.; Rao, V.V.R.N. Structural and electrical studies of sodium iodide doped poly(vinyl alcohol) polymer electrolyte films for their application in electrochemical cells. *Ionics* **2007**, *13*, 173–178. [CrossRef]
74. Bhargav, P.B.; Mohan, V.M.; Sharma, A.K.; Rao, V.V.R.N. Structural and electrical properties of pure and NaBr doped poly (vinyl alcohol) (PVA) polymer electrolyte films for solid-state battery applications. *Ionics* **2007**, *13*, 441–446. [CrossRef]
75. Duraikkan, V.; Sultan, A.B.; Nallaperumal, N.; Shunmuganarayanan, A. Structural, thermal and electrical properties of polyvinyl alcohol/poly(vinyl pyrrolidone)–sodium nitrate solid polymer blend electrolyte. *Ionics* **2018**, *24*, 139–151. [CrossRef]
76. Aziz, S.B.; Nofal, M.M.; Abdulwahid, R.T.; Ghareeb, H.O.; Dannoun, E.M.A.; Abdullah, R.M.; Hamsan, M.H.; Kadir, M.F.Z. Plasticized Sodium-Ion Conducting PVA Based Polymer Electrolyte for Electrochemical Energy Storage—EEC Modeling, Transport Properties, and Charge-Discharge Characteristics. *Polymers* **2021**, *13*, 803. [CrossRef] [PubMed]
77. Khanmirzaei, M.H.; Ramesh, S.; Ramesh, K. Polymer electrolyte based dye-sensitized solar cell with rice starch and 1-methyl-3-propylimidazolium iodide ionic liquid. *Mater. Des.* **2015**, *85*, 833–837. [CrossRef]
78. Binti Shahrudin, S.; Ahmad, A.H. Electrical Analysis of Cornstarch-Based Polymer Electrolyte Doped with NaCl. *Solid State Phenom.* **2017**, *268*, 347–351. [CrossRef]
79. Awang, F.; Hassan, M.; Kamarudin, K. Effect of Sodiumbisulfite on corn starch solid polymer electrolyte. *Malays. J. Anal. Sci.* **2021**, *25*, 224–233.
80. Asnawi, A.S.F.M.; Aziz, S.B.; Brevik, I.; Brza, M.A.; Yusof, Y.M.; Alshehri, S.M.; Ahamad, T.; Kadir, M.F.Z. The Study of Plasticized Sodium-Ion Conducting Polymer Blend Electrolyte Membranes Based on Chitosan/Dextran Biopolymers: Ion Transport, Structural, Morphological and Potential Stability. *Polymers* **2021**, *13*, 383. [CrossRef]

81. Rani, N.S.; Sannappa, J.; Demappa, T.; Mahadevaiah, A. Structural, thermal, and electrical studies of sodium iodide (NaI)-doped hydroxypropyl methylcellulose (HPMC) polymer electrolyte films. *Ionics* **2014**, *20*, 201–207. [CrossRef]
82. Abiddin, J.F.B.; Ahmad, A. Fourier transform infrared spectroscopy and electrical characterization of methylcellulose based solid polymer electrolyte doped with sodium iodide. *J. Teknol.* **2015**, *76*, 41–45.
83. El Sayed, A.M.; Khabiri, G. Spectroscopic, Optical and Dielectric Investigation of (Mg, Cu, Ni, or Cd) Acetates' Influence on Carboxymethyl Cellulose Sodium Salt/Polyvinylpyrrolidone Polymer Electrolyte Films. *J. Electron. Mater.* **2020**, *49*, 2381–2392. [CrossRef]
84. Shetty, S.K.; Ismayil, N.; Shetty, G. Enhancement of Electrical and Optical Properties of Sodium Bromide Doped Carboxymethyl Cellulose Biopolymer Electrolyte Films. *J. Macromol. Sci. Part B* **2020**, *59*, 235–247. [CrossRef]
85. Singh, V.K.; Shalu; Chaurasia, S.K.; Singh, R.K. Development of ionic liquid mediated novel polymer electrolyte membranes for application in Na-ion batteries. *RSC Adv.* **2016**, *6*, 40199–40210. [CrossRef]
86. Zhang, J.; Wen, H.; Yue, L.; Chai, J.; Ma, J.; Hu, P.; Ding, G.; Wang, Q.; Liu, Z.; Cui, G. In Situ Formation of Polysulfonamide Supported Poly(ethylene glycol) Divinyl Ether Based Polymer Electrolyte toward Monolithic Sodium Ion Batteries. *Small* **2017**, *13*, 1601530. [CrossRef] [PubMed]
87. Pan, Q.; Li, Z.; Zhang, W.; Zeng, D.; Sun, Y.; Cheng, H. Single ion conducting sodium ion batteries enabled by a sodium ion exchanged poly(bis(4-carbonyl benzene sulfonyl)imide-co-2,5-diamino benzesulfonic acid) polymer electrolyte. *Solid State Ion.* **2017**, *300*, 60–66. [CrossRef]
88. Chen, S.; Feng, F.; Yin, Y.; Che, H.; Liao, X.-Z.; Ma, Z.-F. A solid polymer electrolyte based on star-like hyperbranched β-cyclodextrin for all-solid-state sodium batteries. *J. Power Sources* **2018**, *399*, 363–371. [CrossRef]
89. Janakiraman, S.; Surendran, A.; Biswal, R.; Ghosh, S.; Anandhan, S.; Venimadhav, A. Electrospun electroactive polyvinylidene fluoride-based fibrous polymer electrolyte for sodium ion batteries. *Mater. Res. Express* **2019**, *6*, 086318. [CrossRef]
90. Yang, J.; Zhang, M.; Chen, Z.; Du, X.; Huang, S.; Tang, B.; Dong, T.; Wu, H.; Yu, Z.; Zhang, J. Flame-retardant quasi-solid polymer electrolyte enabling sodium metal batteries with highly safe characteristic and superior cycling stability. *Nano Res.* **2019**, *12*, 2230–2237. [CrossRef]
91. Liu, K.; Xie, Y.; Yang, Z.; Kim, H.-K.; Dzwiniel, T.L.; Yang, J.; Xiong, H.; Liao, C. Design of a Single-Ion Conducting Polymer Electrolyte for Sodium-Ion Batteries. *J. Electrochem. Soc.* **2021**, *168*, 120543. [CrossRef]
92. Law, H.M.; Yu, J.; Kwok, S.C.T.; Zhou, G.; Robson, M.J.; Wu, J.; Ciucci, F. A hybrid dual-salt polymer electrolyte for sodium metal batteries with stable room temperature cycling performance. *Energy Storage Mater.* **2022**, *46*, 182–191. [CrossRef]
93. Martinez-Cisneros, C.S.; Pandit, B.; Levenfeld, B.; Varez, A.; Sanchez, J.-Y. Flexible solvent-free polymer electrolytes for solid-state Na batteries. *J. Power Sources* **2023**, *559*, 232644. [CrossRef]
94. Olmedo-Martínez, J.L.; Fdz De Anastro, A.; Martínez-Ibañez, M.; Müller, A.J.; Mecerreyes, D. Polyethylene Oxide/Sodium Sulfonamide Polymethacrylate Blends as Highly Conducting Single-Ion Solid Polymer Electrolytes. *Energy Fuels* **2023**, *37*, 5519–5529. [CrossRef]
95. Cheng, X.; Pan, J.; Zhao, Y.; Liao, M.; Peng, H. Gel Polymer Electrolytes for Electrochemical Energy Storage. *Adv. Energy Mater.* **2018**, *8*, 1702184. [CrossRef]
96. Feuillade, G.; Perche, P. Ion-conductive macromolecular gels and membranes for solid lithium cells. *J. Appl. Electrochem.* **1975**, *5*, 63–69. [CrossRef]
97. Baskoro, F.; Wong, H.Q.; Yen, H.-J. Strategic Structural Design of a Gel Polymer Electrolyte toward a High Efficiency Lithium-Ion Battery. *ACS Appl. Energy Mater.* **2019**, *2*, 3937–3971. [CrossRef]
98. Liang, S.; Yan, W.; Wu, X.; Zhang, Y.; Zhu, Y.; Wang, H.; Wu, Y. Gel polymer electrolytes for lithium ion batteries: Fabrication, characterization and performance. *Solid State Ion.* **2018**, *318*, 2–18. [CrossRef]
99. Hsueh, M.-F.; Huang, C.-W.; Wu, C.-A.; Kuo, P.-L.; Teng, H. The Synergistic Effect of Nitrile and Ether Functionalities for Gel Electrolytes Used in Supercapacitors. *J. Phys. Chem. C* **2013**, *117*, 16751–16758. [CrossRef]
100. Ostrovskii, D.; Brodin, A.; Torell, L.M.; Appetecchi, G.B.; Scrosati, B. Molecular and ionic interactions in poly(acrylonitrile)- and poly(methylmetacrylate)-based gel electrolytes. *J. Chem. Phys.* **1998**, *109*, 7618–7624. [CrossRef]
101. Zhu, M.; Wu, J.; Wang, Y.; Song, M.; Long, L.; Siyal, S.H.; Yang, X.; Sui, G. Recent advances in gel polymer electrolyte for high-performance lithium batteries. *J. Energy Chem.* **2019**, *37*, 126–142. [CrossRef]
102. Vincent, C.A. Applications of electroactive polymers. Edited by B. Scrosati. Chapman and Hall, London, 1993. pp. 354 price £40.00. ISBN 0-412-41430-9. *Polym. Int.* **1994**, *33*, 343. [CrossRef]
103. Sannier, L.; Bouchet, R.; Rosso, M.; Tarascon, J.M. Evaluation of GPE performances in lithium metal battery technology by means of simple polarization tests. *J. Power Sources* **2006**, *158*, 564–570. [CrossRef]
104. Groce, F.; Gerace, F.; Dautzemberg, G.; Passerini, S.; Appetecchi, G.B.; Scrosati, B. Synthesis and characterization of highly conducting gel electrolytes. *Electrochim. Acta* **1994**, *39*, 2187–2194. [CrossRef]
105. Hashmi, S.A.; Kumar, A.; Tripathi, S.K. Experimental studies on poly methyl methacrylate-based gel polymer electrolytes for application in electrical double layer capacitors. *J. Phys. D Appl. Phys.* **2007**, *40*, 6527. [CrossRef]
106. Michot, T.; Nishimoto, A.; Watanabe, M. Electrochemical properties of polymer gel electrolytes based on poly(vinylidene fluoride) copolymer and homopolymer. *Electrochim. Acta* **2000**, *45*, 1347–1360. [CrossRef]
107. Stallworth, P.E.; Greenbaum, S.G.; Croce, F.; Slane, S.; Salomon, M. Lithium-7 NMR and ionic conductivity studies of gel electrolytes based on poly(methylmethacrylate). *Electrochim. Acta* **1995**, *40*, 2137–2141. [CrossRef]

108. Karuppasamy, K.; Theerthagiri, J.; Vikraman, D.; Yim, C.-J.; Hussain, S.; Sharma, R.; Maiyalagan, T.; Qin, J.; Kim, H.-S. Ionic Liquid-Based Electrolytes for Energy Storage Devices: A Brief Review on Their Limits and Applications. *Polymers* **2020**, *12*, 918. [CrossRef]
109. Wang, X.; Liu, Z.; Wang, Y.; Chen, J.; Mao, Z.; Wang, D. Conductive $Na_2Zn_2TeO_6$ Filler Modified Gel Polymer Electrolyte Membranes for Application in Sodium-Ions Batteries. *ChemElectroChem* **2020**, *7*, 5021–5028. [CrossRef]
110. Wang, P.; Zhang, H.; Chai, J.; Liu, T.; Hu, R.; Zhang, Z.; Li, G.; Cui, G. A novel single-ion conducting gel polymer electrolyte based on polymeric sodium tartaric acid borate for elevated-temperature sodium metal batteries. *Solid State Ion.* **2019**, *337*, 140–146. [CrossRef]
111. Wang, X.; Wang, X.; Chen, J.; Zhao, Y.; Mao, Z.; Wang, D. Durable sodium battery composed of conductive $Ti_3C_2T_x$ MXene modified gel polymer electrolyte. *Solid State Ion.* **2021**, *365*, 115655. [CrossRef]
112. Vo, D.T.; Do, H.N.; Nguyen, T.T.; Nguyen, T.T.H.; Tran, V.M.; Okada, S.; Le, M.L.P. Sodium ion conducting gel polymer electrolyte using poly(vinylidene fluoride hexafluoropropylene). *Mater. Sci. Eng. B* **2019**, *241*, 27–35. [CrossRef]
113. Harshlata; Mishra, K.; Rai, D.K. Studies on ionic liquid-based nanocomposite gel polymer electrolyte and its application in sodium battery. *Mater. Sci. Eng. B* **2021**, *267*, 115098. [CrossRef]
114. Chen, G.; Zhang, K.; Liu, Y.; Ye, L.; Gao, Y.; Lin, W.; Xu, H.; Wang, X.; Bai, Y.; Wu, C. Flame-retardant gel polymer electrolyte and interface for quasi-solid-state sodium ion batteries. *Chem. Eng. J.* **2020**, *401*, 126065. [CrossRef]
115. Komaba, S.; Ishikawa, T.; Yabuuchi, N.; Murata, W.; Ito, A.; Ohsawa, Y. Fluorinated Ethylene Carbonate as Electrolyte Additive for Rechargeable Na Batteries. *ACS Appl. Mater. Interfaces* **2011**, *3*, 4165–4168. [CrossRef]
116. Shen, W.; Li, H.; Guo, Z.; Wang, C.; Li, Z.; Xu, Q.; Liu, H.; Wang, Y.; Xia, Y. Double-Nanocarbon Synergistically Modified $Na_3V_2(PO_4)_3$: An Advanced Cathode for High-Rate and Long-Life Sodium-Ion Batteries. *ACS Appl. Mater. Interfaces* **2016**, *8*, 15341–15351. [CrossRef] [PubMed]
117. Lonchakova, O.V.; Semenikhin, O.A.; Zakharkin, M.V.; Karpushkin, E.A.; Sergeyev, V.G.; Antipov, E.V. Efficient gel-polymer electrolyte for sodium-ion batteries based on poly(acrylonitrile-co-methyl acrylate). *Electrochim. Acta* **2020**, *334*, 135512. [CrossRef]
118. Tian, L.-Y.; Huang, X.-B.; Tang, X.-Z. Single-ionic gel polymer electrolyte based on polyvinylidene fluoride and fluorine-containing ionomer. *Eur. Polym. J.* **2004**, *40*, 735–742. [CrossRef]
119. Parveen, S.; Sehrawat, P.; Hashmi, S.A. Triglyme-based solvate ionic liquid gelled in a polymer: A novel electrolyte composition for sodium-ion battery. *Mater. Today Commun.* **2022**, *31*, 103392. [CrossRef]
120. Van Nghia, N.; Long, P.D.; Tan, T.A.; Jafian, S.; Hung, I.M. Electrochemical Performance of a V_2O_5 Cathode for a Sodium Ion Battery. *J. Electron. Mater.* **2017**, *46*, 3689–3694. [CrossRef]
121. Kumar, D.; Hashmi, S.A. Ionic liquid based sodium ion conducting gel polymer electrolytes. *Solid State Ion.* **2010**, *181*, 416–423. [CrossRef]
122. Kumar, D.; Yadav, N.; Mishra, K.; Shahid, R.; Arif, T.; Kanchan, D.K. Sodium ion conducting flame-retardant gel polymer electrolyte for sodium batteries and electric double layer capacitors (EDLCs). *J. Energy Storage* **2022**, *46*, 103899. [CrossRef]
123. Mishra, R.; Singh, S.K.; Gupta, H.; Tiwari, R.K.; Meghnani, D.; Patel, A.; Tiwari, A.; Tiwari, V.K.; Singh, R.K. Polar β-Phase PVdF-HFP-Based Freestanding and Flexible Gel Polymer Electrolyte for Better Cycling Stability in a Na Battery. *Energy Fuels* **2021**, *35*, 15153–15165. [CrossRef]
124. Mishra, K.; Garg, A.; Sharma, R.; Gautam, R.; Pundir, S.S. Effect of blending of PMMA on PVdF-HFP + $NaCF_3SO_3$-EC-PC gel polymer electrolyte. *Mater. Today Proc.* **2019**, *12*, 621–627. [CrossRef]
125. Chauhan, A.K.; Kumar, D.; Mishra, K.; Singh, A. Performance enhancement of Na^+ ion conducting porous gel polymer electrolyte using $NaAlO_2$ active filler. *Mater. Today Commun.* **2021**, *26*, 101713. [CrossRef]
126. Janakiraman, S.; Agrawal, A.; Biswal, R.; Venimadhav, A. An amorphous polyvinylidene fluoride-co-hexafluoropropylene based gel polymer electrolyte for sodium-ion cells. *Appl. Surf. Sci. Adv.* **2021**, *6*, 100139. [CrossRef]
127. Janakiraman, S.; Padmaraj, O.; Ghosh, S.; Venimadhav, A. A porous poly (vinylidene fluoride-co-hexafluoropropylene) based separator-cum-gel polymer electrolyte for sodium-ion battery. *J. Electroanal. Chem.* **2018**, *826*, 142–149. [CrossRef]
128. Yang, L.; Jiang, Y.; Liang, X.; Lei, Y.; Yuan, T.; Lu, H.; Liu, Z.; Cao, Y.; Feng, J. Novel Sodium–Poly(tartaric acid)Borate-Based Single-Ion Conducting Polymer Electrolyte for Sodium–Metal Batteries. *ACS Appl. Energy Mater.* **2020**, *3*, 10053–10060. [CrossRef]
129. Feng, J.; An, Y.; Ci, L.; Xiong, S. Nonflammable electrolyte for safer non-aqueous sodium batteries. *J. Mater. Chem. A* **2015**, *3*, 14539–14544. [CrossRef]
130. Liu, X.; Jiang, X.; Zhong, F.; Feng, X.; Chen, W.; Ai, X.; Yang, H.; Cao, Y. High-Safety Symmetric Sodium-Ion Batteries Based on Nonflammable Phosphate Electrolyte and Double $Na_3V_2(PO_4)_3$ Electrodes. *ACS Appl. Mater. Interfaces* **2019**, *11*, 27833–27838. [CrossRef]
131. Park, T.-H.; Park, M.-S.; Ban, A.H.; Lee, Y.-S.; Kim, D.-W. Nonflammable Gel Polymer Electrolyte with Ion-Conductive Polyester Networks for Sodium Metal Cells with Excellent Cycling Stability and Enhanced Safety. *ACS Appl. Energy Mater.* **2021**, *4*, 10153–10162. [CrossRef]
132. Niu, Y.-B.; Yin, Y.-X.; Wang, W.-P.; Wang, P.-F.; Ling, W.; Xiao, Y.; Guo, Y.-G. In Situ Copolymerizated Gel Polymer Electrolyte with Cross-Linked Network for Sodium-Ion Batteries. *CCS Chem.* **2020**, *2*, 589–597. [CrossRef]
133. Farhana, N.K.; Khanmirzaei, M.H.; Ramesh, S.; Ramesh, K. Exploration on polypropylene carbonate polymer for gel polymer electrolyte preparation and dye-sensitized solar cell application. *J. Appl. Polym. Sci.* **2017**, *134*, 45091. [CrossRef]

134. Krishna Jyothi, N.; Vijaya Kumar, K.; Sunita Sundari, G.; Narayana Murthy, P. Ionic conductivity and battery characteristic studies of a new PAN-based Na^+ ion conducting gel polymer electrolyte system. *Indian J. Phys.* **2016**, *90*, 289–296. [CrossRef]
135. Zhang, Y.; Bakenov, Z.; Tan, T.; Huang, J. Polyacrylonitrile-Nanofiber-Based Gel Polymer Electrolyte for Novel Aqueous Sodium-Ion Battery Based on a $Na_4Mn_9O_{18}$ Cathode and Zn Metal Anode. *Polymers* **2018**, *10*, 853. [CrossRef]
136. Mei, W.; Wang, X.; Wang, Y.; Chen, J.; Mao, Z.; Wang, D. Conductive $Na_3Sc_2P_3O_{12}$ filler with different crystal phases modified gel polymer electrolyte membranes for sodium ions batteries. *J. Solid State Chem.* **2021**, *302*, 122459. [CrossRef]
137. Boehm, L.; Delbecq, C.J.; Hutchinson, E.; Susman, S. Fast ion conduction and phase transitions in various preparations of $Na_3Sc_2P_3O_{12}$. *Solid State Ion.* **1981**, *5*, 311–314. [CrossRef]
138. Kim, J.I.; Chung, K.Y.; Park, J.H. Design of a porous gel polymer electrolyte for sodium-ion batteries. *J. Membr. Sci.* **2018**, *566*, 122–128. [CrossRef]
139. Kim, H.W.; Kim, H.-J.; Byeon, H.; Kim, J.; Yang, J.W.; Kim, Y.; Kim, J.-K. Binder-free organic cathode based on nitroxide radical polymer-functionalized carbon nanotubes and gel polymer electrolyte for high-performance sodium organic polymer batteries. *J. Mater. Chem. A* **2020**, *8*, 17980–17986. [CrossRef]
140. Shin, W.-K.; Cho, J.; Kannan, A.G.; Lee, Y.-S.; Kim, D.-W. Cross-linked Composite Gel Polymer Electrolyte using Mesoporous Methacrylate-Functionalized SiO_2 Nanoparticles for Lithium-Ion Polymer Batteries. *Sci. Rep.* **2016**, *6*, 26332. [CrossRef]
141. Aravindan, V.; Vickraman, P.; Sivashanmugam, A.; Thirunakaran, R.; Gopukumar, S. Comparison among the performance of LiBOB, LiDFOB and LiFAP impregnated polyvinylidenefluoride-hexafluoropropylene nanocomposite membranes by phase inversion for lithium batteries. *Curr. Appl. Phys.* **2013**, *13*, 293–297. [CrossRef]
142. Shim, J.; Kim, H.J.; Kim, B.G.; Kim, Y.S.; Kim, D.-G.; Lee, J.-C. 2D boron nitride nanoflakes as a multifunctional additive in gel polymer electrolytes for safe, long cycle life and high rate lithium metal batteries. *Energy Environ. Sci.* **2017**, *10*, 1911–1916. [CrossRef]
143. Zhao, Y.; Liu, H.; Meng, X.; Liu, A.; Chen, Y.; Ma, T. A cross-linked tin oxide/polymer composite gel electrolyte with adjustable porosity for enhanced sodium-ion batteries. *Chem. Eng. J.* **2022**, *431*, 133922. [CrossRef]
144. Shi, J.; Xiong, H.; Yang, Y.; Shao, H. Nano-sized oxide filled composite PEO/PMMA/P(VDF-HFP) gel polymer electrolyte for rechargeable lithium and sodium batteries. *Solid State Ion.* **2018**, *326*, 136–144. [CrossRef]
145. Dong, T.; Zhang, J.; Xu, G.; Chai, J.; Du, H.; Wang, L.; Wen, H.; Zang, X.; Du, A.; Jia, Q. A multifunctional polymer electrolyte enables ultra-long cycle-life in a high-voltage lithium metal battery. *Energy Environ. Sci.* **2018**, *11*, 1197–1203. [CrossRef]
146. Zhu, Y.; Yang, Y.; Fu, L.; Wu, Y. A porous gel-type composite membrane reinforced by nonwoven: Promising polymer electrolyte with high performance for sodium-ion batteries. *Electrochim. Acta* **2017**, *224*, 405–411. [CrossRef]
147. Pu, W.; He, X.; Wang, L.; Jiang, C.; Wan, C. Preparation of PVDF–HFP microporous membrane for Li-ion batteries by phase inversion. *J. Membr. Sci.* **2006**, *272*, 11–14. [CrossRef]
148. Evans, J.; Vincent, C.A.; Bruce, P.G. Electrochemical measurement of transference numbers in polymer electrolytes. *Polymer* **1987**, *28*, 2324–2328. [CrossRef]
149. Lei, D.; He, Y.-B.; Huang, H.; Yuan, Y.; Zhong, G.; Zhao, Q.; Hao, X.; Zhang, D.; Lai, C.; Zhang, S. Cross-linked beta alumina nanowires with compact gel polymer electrolyte coating for ultra-stable sodium metal battery. *Nat. Commun.* **2019**, *10*, 4244. [CrossRef] [PubMed]
150. Kumar, D.; Hashmi, S.A. Ion transport and ion–filler-polymer interaction in poly(methyl methacrylate)-based, sodium ion conducting, gel polymer electrolytes dispersed with silica nanoparticles. *J. Power Sources* **2010**, *195*, 5101–5108. [CrossRef]
151. Kim, J.I.; Choi, Y.; Chung, K.Y.; Park, J.H. A Structurable Gel-Polymer Electrolyte for Sodium Ion Batteries. *Adv. Funct. Mater.* **2017**, *27*, 1701768. [CrossRef]
152. Gao, H.; Guo, B.; Song, J.; Park, K.; Goodenough, J.B. A Composite Gel–Polymer/Glassfiber Electrolyte for Sodium-Ion Batteries. *Adv. Energy Mater.* **2015**, *5*, 1402235. [CrossRef]
153. Wang, L.; Lu, Y.; Liu, J.; Xu, M.; Cheng, J.; Zhang, D.; Goodenough, J.B. A Superior Low-Cost Cathode for a Na-Ion Battery. *Angew. Chem. Int. Ed.* **2013**, *52*, 1964–1967. [CrossRef]
154. Park, K.; Cho, J.H.; Shanmuganathan, K.; Song, J.; Peng, J.; Gobet, M.; Greenbaum, S.; Ellison, C.J.; Goodenough, J.B. New battery strategies with a polymer/Al_2O_3 separator. *J. Power Sources* **2014**, *263*, 52–58. [CrossRef]
155. Jiang, Y.; Zhou, X.; Li, D.; Cheng, X.; Liu, F.; Yu, Y. Highly Reversible Na Storage in $Na_3V_2(PO_4)_3$ by Optimizing Nanostructure and Rational Surface Engineering. *Adv. Energy Mater.* **2018**, *8*, 1800068. [CrossRef]
156. Luo, C.; Shen, T.; Ji, H.; Huang, D.; Liu, J.; Ke, B.; Wu, Y.; Chen, Y.; Yan, C. Mechanically Robust Gel Polymer Electrolyte for an Ultrastable Sodium Metal Battery. *Small* **2020**, *16*, 1906208. [CrossRef]
157. Luo, C.; Shen, T.; Ke, B.; Wu, Y.; Chen, Y. Ultra-small $Na_3V_2(PO_4)_3$ nanoparticles decorated MOFs-derived carbon enabling fast charge transfer for high-rate sodium storage. *Solid State Ion.* **2019**, *342*, 115061. [CrossRef]
158. Mishra, K.; Arif, T.; Kumar, R.; Kumar, D. Effect of Al_2O_3 nanoparticles on ionic conductivity of PVdF-HFP/PMMA blend-based Na-ion conducting nanocomposite gel polymer electrolyte. *J. Solid State Electrochem.* **2019**, *23*, 2401–2409. [CrossRef]
159. Yao, P.; Yu, H.; Ding, Z.; Liu, Y.; Lu, J.; Lavorgna, M.; Wu, J.; Liu, X. Review on Polymer-Based Composite Electrolytes for Lithium Batteries. *Front. Chem.* **2019**, *7*, 522. [CrossRef]
160. Yabuuchi, N.; Kubota, K.; Dahbi, M.; Komaba, S. Research Development on Sodium-Ion Batteries. *Chem. Rev.* **2014**, *114*, 11636–11682. [CrossRef]

161. Das, S.K.; Mandal, S.S.; Bhattacharyya, A.J. Ionic conductivity, mechanical strength and Li-ion battery performance of mono-functional and bi-functional ("Janus") "soggy sand" electrolytes. *Energy Environ. Sci.* **2011**, *4*, 1391–1399. [CrossRef]
162. Cao, J.; Wang, L.; He, X.; Fang, M.; Gao, J.; Li, J.; Deng, L.; Chen, H.; Tian, G.; Wang, J. In situ prepared nano-crystalline TiO_2–poly(methyl methacrylate) hybrid enhanced composite polymer electrolyte for Li-ion batteries. *J. Mater. Chem. A* **2013**, *1*, 5955–5961. [CrossRef]
163. Croce, F.; Appetecchi, G.B.; Persi, L.; Scrosati, B. Nanocomposite polymer electrolytes for lithium batteries. *Nature* **1998**, *394*, 456–458. [CrossRef]
164. Ni'mah, Y.L.; Cheng, M.-Y.; Cheng, J.H.; Rick, J.; Hwang, B.-J. Solid-state polymer nanocomposite electrolyte of TiO_2/PEO/$NaClO_4$ for sodium ion batteries. *J. Power Sources* **2015**, *278*, 375–381. [CrossRef]
165. Verma, H.; Mishra, K.; Rai, D.K. Sodium ion conducting nanocomposite polymer electrolyte membrane for sodium-ion batteries. *J. Solid State Electrochem.* **2020**, *24*, 521–532. [CrossRef]
166. Zhang, X.; Wang, X.; Liu, S.; Tao, Z.; Chen, J. A novel PMA/PEG-based composite polymer electrolyte for all-solid-state sodium-ion batteries. *Nano Res.* **2018**, *11*, 6244–6251. [CrossRef]
167. Zhang, Z.; Xu, K.; Rong, X.; Hu, Y.-S.; Li, H.; Huang, X.; Chen, L. $Na_{3.4}Zr_{1.8}Mg_{0.2}Si_2PO_{12}$ filled poly(ethylene oxide)/$Na(CF_3SO_2)2N$ as flexible composite polymer electrolyte for solid-state sodium batteries. *J. Power Sources* **2017**, *372*, 270–275. [CrossRef]
168. Jian, Z.; Zhao, L.; Pan, H.; Hu, Y.-S.; Li, H.; Chen, W.; Chen, L. Carbon coated $Na_3V_2(PO_4)_3$ as novel electrode material for sodium ion batteries. *Electrochem. Commun.* **2012**, *14*, 86–89. [CrossRef]
169. Zhang, Z.; Zhang, Q.; Shi, J.; Chu, Y.S.; Yu, X.; Xu, K.; Ge, M.; Yan, H.; Li, W.; Gu, L. A Self-Forming Composite Electrolyte for Solid-State Sodium Battery with Ultralong Cycle Life. *Adv. Energy Mater.* **2017**, *7*, 1601196. [CrossRef]
170. Zhao, Y.; Wang, H.; Gao, G.; Qi, L. Nanofiber membrane based on ionic liquids as high-performance polymer electrolyte for sodium electrochemical device. *Ionics* **2013**, *19*, 1595–1602. [CrossRef]
171. Farmer, V.; Welton, T. The oxidation of alcohols in substituted imidazolium ionic liquids using ruthenium catalysts. *Green Chem.* **2002**, *4*, 97–102. [CrossRef]
172. Raghavan, P.; Zhao, X.; Manuel, J.; Shin, C.; Heo, M.-Y.; Ahn, J.-H.; Ryu, H.-S.; Ahn, H.-J.; Noh, J.-P.; Cho, G.-B. Electrochemical studies on polymer electrolytes based on poly(vinylidene fluoride-co-hexafluoropropylene) membranes prepared by electrospinning and phase inversion—A comparative study. *Mater. Res. Bull.* **2010**, *45*, 362–366. [CrossRef]
173. Song, S.; Dong, Z.; Fernandez, C.; Wen, Z.; Hu, N.; Lu, L. Nanoporous ceramic-poly(ethylene oxide) composite electrolyte for sodium metal battery. *Mater. Lett.* **2019**, *236*, 13–15. [CrossRef]
174. Lee, S.; Park, S.-J.; Kim, S. Thermal and Electrical Conducting Property of Sodium Polymer Electrolyte Containing Barium Titanate Filler. *J. Nanosci. Nanotechnol.* **2017**, *17*, 5768–5770. [CrossRef]
175. Serra Moreno, J.; Armand, M.; Berman, M.B.; Greenbaum, S.G.; Scrosati, B.; Panero, S. Composite PEOn:NaTFSI polymer electrolyte: Preparation, thermal and electrochemical characterization. *J. Power Sources* **2014**, *248*, 695–702. [CrossRef]
176. Perrier, M.; Besner, S.; Paquette, C.; Vallée, A.; Lascaud, S.; Prud'homme, J. Mixed-alkali effect and short-range interactions in amorphous poly(ethylene oxide) electrolytes. *Electrochim. Acta* **1995**, *40*, 2123–2129. [CrossRef]
177. Appetecchi, G.B.; Croce, F.; Dautzenberg, G.; Mastragostino, M.; Ronci, F.; Scrosati, B.; Soavi, F.; Zanelli, A.; Alessandrini, F.; Prosini, P.P. Composite Polymer Electrolytes with Improved Lithium Metal Electrode Interfacial Properties: I. Elechtrochemical Properties of Dry PEO-Li_X Systems. *J. Electrochem. Soc.* **1998**, *145*, 4126. [CrossRef]
178. Kunteppa, H.; Roy, A.S.; Koppalkar, A.R.; Ambika Prasad, M.V.N. Synthesis and morphological change in poly(ethylene oxide)–sodium chlorate based polymer electrolyte complex with polyaniline. *Phys. B Condens. Matter* **2011**, *406*, 3997–4000. [CrossRef]
179. Chen, S.; Feng, F.; Che, H.; Yin, Y.; Ma, Z.-F. High-performance solid-state sodium batteries enabled by boron-contained 3D composite polymer electrolyte. *Chem. Eng. J.* **2021**, *406*, 126736. [CrossRef]
180. Sun, L.; Xie, Y.; Liao, X.-Z.; Wang, H.; Tan, G.; Chen, Z.; Ren, Y.; Gim, J.; Tang, W.; He, Y.-S. Insight into Ca-Substitution Effects on O_3-Type $NaNi_1/3Fe_1/3Mn_1/3O_2$ Cathode Materials for Sodium-Ion Batteries Application. *Small* **2018**, *14*, 1704523. [CrossRef]
181. Chen, S.; Che, H.; Feng, F.; Liao, J.; Wang, H.; Yin, Y.; Ma, Z.-F. Poly(vinylene carbonate)-Based Composite Polymer Electrolyte with Enhanced Interfacial Stability To Realize High-Performance Room-Temperature Solid-State Sodium Batteries. *ACS Appl. Mater. Interfaces* **2019**, *11*, 43056–43065. [CrossRef]
182. Ahad, N.; Saion, E.; Gharibshahi, E. Structural, Thermal, and Electrical Properties of PVA-Sodium Salicylate Solid Composite Polymer Electrolyte. *J. Nanomater.* **2012**, *2012*, 857569. [CrossRef]
183. Yu, X.; Xue, L.; Goodenough, J.B.; Manthiram, A. A High-Performance All-Solid-State Sodium Battery with a Poly(ethylene oxide)–$Na_3Zr_2Si_2PO_{12}$ Composite Electrolyte. *ACS Mater. Lett.* **2019**, *1*, 132–138. [CrossRef]
184. Wang, Y.; Wang, Z.; Zheng, F.; Sun, J.; Oh, J.A.S.; Wu, T.; Chen, G.; Huang, Q.; Kotobuki, M.; Zeng, K. Ferroelectric Engineered Electrode-Composite Polymer Electrolyte Interfaces for All-Solid-State Sodium Metal Battery. *Adv. Sci.* **2022**, *9*, 2105849. [CrossRef]
185. Wang, Y.; Wang, Z.; Sun, J.; Zheng, F.; Kotobuki, M.; Wu, T.; Zeng, K.; Lu, L. Flexible, stable, fast-ion-conducting composite electrolyte composed of nanostructured Na-super-ion-conductor framework and continuous Poly(ethylene oxide) for all-solid-state Na battery. *J. Power Sources* **2020**, *454*, 227949. [CrossRef]
186. Wang, Y.; Yao, K.; Sharifzadeh Mirshekarloo, M.; Tay, F.E.H. Effects and Mechanism of Combinational Chemical Agents on Solution-Derived $K0.5Na0.5NbO_3$ Piezoelectric Thin Films. *J. Am. Ceram. Soc.* **2016**, *99*, 1631–1636. [CrossRef]

187. Dimri, M.C.; Kumar, D.; Aziz, S.B.; Mishra, K. $ZnFe_2O_4$ nanoparticles assisted ion transport behavior in a sodium ion-conducting polymer electrolyte. *Ionics* **2021**, *27*, 1143–1157. [CrossRef]
188. Chauhan, A.K.; Mishra, K.; Kumar, D.; Singh, A. Enhancing Sodium Ion Transport in a PEO-Based Solid Polymer Electrolyte System with $NaAlO_2$ Active Fillers. *J. Electron. Mater.* **2021**, *50*, 5122–5133. [CrossRef]
189. Yao, Y.; Liu, Z.; Wang, X.; Chen, J.; Wang, X.; Wang, D.; Mao, Z. Promoted ion conductivity of sodium salt–poly(ethylene oxide) polymer electrolyte induced by adding conductive beta-alumina and application in all-solid-state sodium batteries. *J. Mater. Sci.* **2021**, *56*, 9951–9960. [CrossRef]
190. Mallaiah, Y.; Jeedi, V.R.; Swarnalatha, R.; Raju, A.; Narender Reddy, S.; Sadananda Chary, A. Impact of polymer blending on ionic conduction mechanism and dielectric properties of sodium based PEO-PVdF solid polymer electrolyte systems. *J. Phys. Chem. Solids* **2021**, *155*, 110096. [CrossRef]
191. Pradhan, D.K.; Samantaray, B.K.; Choudhary, R.N.P.; Thakur, A.K. Effect of plasticizer on microstructure and electrical properties of a sodium ion conducting composite polymer electrolyte. *Ionics* **2005**, *11*, 95–102. [CrossRef]